SYNTHESIS OF SILVER NANOPARTICLES AND CABLE LIKE
STRUCTURES THROUGH COAXIAL ELECTROSPINNING

A THESIS SUBMITTED TO
THE GRADUATE SCHOOL OF NATURAL AND APPLIED SCIENCES
OF
MIDDLE EAST TECHNICAL UNIVERSITY

BY

SİMGE ÇINAR

IN PARTIAL FULFILLMENT OF THE REQUIREMENTS
FOR
THE DEGREE OF MASTER OF SCIENCE
IN
CHEMICAL ENGINEERING

DECEMBER 2009

Approval of the thesis:

SYNTHESIS OF SILVER NANOPARTICLES AND CABLE LIKE STRUCTURES THROUGH COAXIAL ELECTROSPINNING

submitted by **SİMGE ÇINAR** in partial fulfillment of the requirements for the degree of **Master of Science in Chemical Engineering Department, Middle East Technical University** by,

Prof. Dr. Canan Özgen _____
Dean, Graduate School of **Natural and Applied Sciences**

Prof. Dr. Gürkan Karakaş _____
Head of Dept., **Chemical Engineering**

Prof. Dr. Güngör Gündüz _____
Supervisor, **Chemical Engineering Dept., METU**

Prof. Dr. Üner Çolak _____
Co-Supervisor, **Nuclear Energy Engineering Dept., HU**

Examining Committee Members:

Prof. Dr. H. Önder Özbelge _____
Chemical Engineering Dept., METU

Prof. Dr. Güngör Gündüz _____
Chemical Engineering Dept., METU

Prof. Dr. Şakir Erkoç _____
Physics Dept., METU

Assoc. Prof. Dr. Göknur Bayram _____
Chemical Engineering Dept., METU

Asst. Prof. Dr. H. Emrah Ünalan _____
Metallurgical and Materials Engineering Dept., METU

Date: 30/12/2009

I hereby declare that all information in this document has been obtained and presented in accordance with academic rules and ethical conduct. I also declare that, as required by these rules and conduct, I have fully cited and referenced all material and results that are not original to this work.

Name, Last name: Simge Çınar

Signature   :

ABSTRACT

SYNTHESIS OF SILVER NANOPARTICLES, AND CABLE LIKE STRUCTURES THROUGH COAXIAL ELECTROSPINNING

Çınar, Simge

M.S., Department of Chemical Engineering

Supervisor: Prof. Dr. Güngör Gündüz

Co-Supervisor: Prof. Dr. Üner Çolak

December 2009, 91 pages

The aim of this study is to demonstrate the possibility of production of nanocables as an alternative to the other one dimensional metal/polymer composite structures like nanowires and nanorods. There is no certain definition of nanocables; however they could be considered as assemblies of nanowires. Nanocable structure can be defined as a core-shell structure formed by a polymeric shell and a metal core that runs continuously within this shell. To produce nanocables, two main steps were carried out. Firstly, monodispersed silver metal nanoparticles to be aligned within the cable core were produced. Investigations on reduction reactions in the presence of

strong and weak reducing agents and different capping agents revealed the importance of the kinetics of reduction in the production of monodispersed nanoparticles. Use of capping agents to give a positive reduction potential, resulted in the slow reduction rates that was critical for fine tuning of the final particle sizes between 1-10 nm. Hydrazine hydrate and oleylamine/ oleic acid systems were used as strong and weak reducing agents, respectively. By using weak reducing agent, monodisperse spherical silver nanoparticles with the diameter of 2.7 nm were produced. It was shown that particles with controlled diameter and size distribution can be obtained by tuning the system parameters. Secondly, particles produced as such were electrospun within the core of the polymer nanofibers and long continuous nanocables were produced. Polyvinyl pyrrolidone and polycaprolactone were used in shell part of nanocables. Transmission electron microscopy (TEM), scanning electron microscopy (SEM), photon correlation spectroscopy (PCS), X-ray diffraction (XRD) and surface plasmon resonance spectroscopy (SPR) analyses were carried out in order to understand the mechanism by which the nanoparticles were reduced and for further characterization of the product.

Keywords: Metal/Polymer Nanocomposite, Nanocable, Silver, Metal Nanoparticle, Oleylamine, Oleic acid, Hydrazine Hydrate, Coaxial Electrospinning

ÖZ

GÜMÜŞ NANOPARÇACIKLARININ VE KABLO BENZERİ YAPILARIN EŞEKSENLİ ELEKTROEĞİRME YÖNTEMİ İLE ÜRETİMİ

Çınar, Simge

Yüksek Lisans, Kimya Mühendisliği Bölümü

Tez Yöneticisi: Prof. Dr. Güngör Gündüz

Ortak Tez Yöneticisi: Prof. Dr. Üner Çolak

Aralık 2009, 91 sayfa

Bu çalışmanın amacı, diğer bir boyutlu metal/polimer kompozit yapılarına bir seçenek olarak nanokablo yapıları üetmektir. Bu yapılar, nanotellerin bir araya getirilerek oluşturdukları yapılar olarak düşünülebilir. Metal çekirdek üzerine polimer kılıf çevrilerek oluşturulmuş lif yapı, eşeksenli electroeğirme yöntemi ile elde edilmiştir. Nano kablo yapılarının oluşturulması iki temel aşamada gerçekleştirilmiştir. İlk olarak liflerin çekirdek kısmında dizilecek tek boyut dağılımlı metal nano parçacıkları üretilmiştir. Kuvvetli ve zayıf indirgeyici ajanlar ile farklı koruyucu kılıflar üzerine yapılan araştırmalar, metal parçacıkların üretiminde indirgenme tepkimelerinin önemini ortaya çıkarmıştır. İndirgenme tepkimeleri için

gerekli potansiyeli düşüren koruyucu kılıflar, indirgenme tepkimelerini yavaşlatarak, boyutları 1-10 nm arasında ayarlanabilen parçacık üretimini mümkün kılmaktadırlar. Hidrizin hidrat ve oleilamin/oleik asit sırasıyla kuvvetli ve zayıf indirgenme ajanları olarak kullanılmıştır. Zayıf ajanlar kullanıldığında, ortalama 2.7nm çapında, tek boyut dağılımlı, dairesel gümüş parçacıkları üretilmiştir. Sistem değişkenlerinin düzenlenmesi ile istenilen parçacık boyut ve dağılımında parçacıklar üretilebileceği de gösterilmiştir. İkinci basamak olarak üretilen bu parçacıklar polimer liflerin içerisinde elektroeğrilmiş ve uzun, devamlı nanokablo yapılar üretilebilmiştir. Nano kablo yapılarda kılıf olarak polivinil pyrolidon ve polikaprolakton kullanılmıştır. Nanoparçacıkların oluşum mekanızmasını anlayabilmek ve ürünleri karakterize edebilmek için geçirmeli elektron mikroskobu (TEM), taramalı elektron mikroskobu (SEM), foton korelasyon spektroskopisi (PCS), X-ray ışık kırılım cihazı (XRD) and UV-Vis analizleri yapılmıştır.

Anahtar sözcükler: Metal/Polimer Kompozit, Nanokablo, Gümüş, Metal Nano Parçacık, Oleilamin, Hidrazin Hidrat, Eşeksenli Elektroeğirme

To My Mother,

ACKNOWLEDGEMENTS

TABLE OF CONTENTS

LIST OF TABLES

LIST OF FIGURES

FIGURES

LIST OF SYMBOLS AND ABBREVIATIONS

CMC   Critical Micelle Concentration

DC   Direct Current

DMF   N,N-Dimethylformamide

DSS   Dioctlyl Sulfosuccinate Sodium Salt

ES   Electrospinning

FWHM   Full Width at Half Maximum

g   Gram

HH   Hydrazine Hydrate

HEOS   Hexane Evaporated Optimized Solution

h   Hour

K_b Dissociation Constant

kV   Kilovolt

m   Meter

ml   Milliliter

mm   Millimeter

mmol   Millimole

min   Minute

M   Molarity

nm   Nanometer

OAc   Oleic Acid

OAm   Oleylamine

OS   Optimized Solution

PCL   Poly (Caprolactone)

PCS	Photon Correlation Spectroscopy
PVA	Poly (Vinyl Alcohol)
PVP	Poly (Vinyl Pyrrolidone)
rpm	Revolutions per Minute
SEM	Scanning Electron Spectroscopy
SPR	Surface Plasmon Resonance
TEM	Transmission Electron Spectroscopy
UV-vis	Ultraviolet – Visible Spectroscopy
V	Volt
wt	Weight
XRD	X-Ray Diffractometer
$E°_{red}$	Reduction Potential
μm	Micrometer
°	Degree
°C	Celsius Degree

CHAPTER 1

INTRODUCTION

Developments in technology arise the need for novel functional materials. Materials in nano-scale are one of the best candidates to supply this due to their unique properties. When nano-sized phase combined with the other nano or bulk phase, nanocomposite materials form, and thus different functionalities of the phases become integrated in a single material.

Metal-polymer nanocomposites are novel materials which may overcome the demand in many applications such as catalysis, photography, electronics, photonics, information storage, optoelectronics, biological labeling, imaging, sensing, etc. By controlling the size, shape, composition, crystallinity, and structure of materials, their properties can be adjusted according to the need. Shape controllability attracts special interest among the others due to versatile tuning of properties [1]. Different shaped nano gold and silver particles are considered to be used in detection and treatment of cancer due to their different surface plasmon resonance, which refers to the characteristic wavelength at which free electrons in a

1

nanomaterial collectively oscillate and scatter/absorb an incident electromagnetic wave [1].

Another shape, therefore, functionality dependent application is gold and silver nanowires. They are considered as an essential component of molecular scale interconnects to achieve extremely dense logic and memory circuits due to their high conductivity [2].

Nanowires received special interest in recent years due to their one dimensional structure. According to the synthesis methodology, wire properties differ. Ligand control and oriented arrangement are common methodologies. Wires produced by certain orientation process, i.e. self assembly, and colloidal stability, have predetermined size and monodispersity, and rather constant diameter during growth. However, only the production of small quantities is possible by this method. The mechanism of the system is not well understood and the product contains impurities. On the other hand, procedure with ligand control makes the large quantity production possible with colloidal stability; however, again purity is a problem [3].

Impurity problem is originated from the necessity of using capping agents during production. Otherwise, extremely small metal particles aggregate due to their high surface energy, and be oxidized and contaminated by air, moisture, etc. Capping agents also gives the capability of self assembly to the system. Therefore, it is not reasonable to totally remove capping agent from the system; however,

minimizing the amount could provide an adequate solution. Another problem with the nanowires is their length. Whichever method is used, wires lengths are always limited to few μm and interconnection of these wires and using them for their conduction become another problem.

In this study, the methodology to produce nanocables is analyzed. There is no certain definition of nanocables in the literature; however, the closest structures resembling nanocables are nanorods and nanowires. Diameters of nanowires and nanorods are commonly between 1 and 100 nm. They differ in terms of their aspect ratio. The aspect ratio of nanorods is between 1 and 20, whereas, it is greater than 20 for nanowires. [4] Nanocable is the core-sheath structured form of nanofibers (Figure1.1). They could be considered like assemblies of nanowires. By coaxial electrospinning, orientation of metal particles can be obtained in fiber formation step. Due to protective polymer shell, oxidation and contamination of the metal core can be prevented. Denser metal particles can be placed into fibers minimizing the amount of required metal nanoparticles.
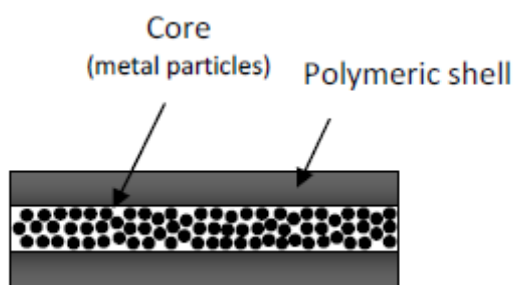
Figure 1.1 Nanocable structure

There are many studies in literature about acquiring of metal nanoparticle. Gold (Au), palladium (Pd), silver (Ag), and copper (Cu) are most frequently studied metals due to their unpaired outer shell electrons which enhance their interaction with ions [3, 5-7]. Among these metals, silver not only exhibits very high electrical and thermal conductivities in the bulk form, but also is relatively inexpensive and has good chemical and physical properties [8, 9].

It is hard to classify studies in literature according to certain rules since wide range of chemicals and strategies were used. Chen et al. classified the silver nanoparticle production methods according to reducing agent [10]. In nanoparticle synthesis, reduction process is essentially the most critical step because of its effect on particle size and size distribution. Many examples for the size-shape control problem can be seen in the literature. Although capping agents are used to prevent aggregation, they may not be adequate solution for all cases. If reducing agents are strong enough, they may deform these protective shields.

The importance of reducing agent and reduction mechanism were investigated in detail in the present study by comparing the effect of strong and weak agents for the reduction of silver nitrate. In addition to capping agents, polymer shield was also used in the strong reducing agent system and reduction reaction was tried to be control by reductant addition rate, etc. However, monodispersed spherical silver nanoparticles could be produced only by reaction with weak

reducing agents. Hydrazine hydrate and oleylamine/oleic acid systems were used as strong and weak reducing agent systems, respectively. Reduction mechanisms of these systems were also studied. Following the measurement of particle size, size distribution and morphological characterizations of these particles, they were introduced into the core of the polymer nanofibers by co-axial electrospinning method. Thus, cable like structures were produced. In order to analyze the product and understand the system, transmission electron microscopy (TEM), scanning electron microscopy (SEM), photon correlation spectroscopy (PCS), X-ray diffraction (XRD), and ultraviolet-visible spectroscopy (UV-Vis) analysis were conducted.

CHAPTER 2

LITERATURE REVIEW

2.1 METAL NANOPARTICLE FORMATION

The properties of the metal nanoparticles differ according to their shape, size, composition, crystallinity and structure allowing to unlimited combinations of properties and synthesis recipies. In any case, all of these systems should contain metal precursor, reducing agent, and a stabilizing agent.

There are also some predominant production methods in literature; chemical reduction in aqueous and non-aqueous solutions, template synthesis method, electrochemical or ultrasonic-assisted reduction, photo-induced or photocatalytic reduction, microwave-assisted synthesis, irradiation reduction, microemulsion method, biochemical reduction, etc. [10]. In microwave, irradiation, and photo-inducement methods, reaction occurs very rapidly; however, it is difficult to achieve narrow size distribution of silver particles or clusters. Biological reduction is a promising method due to mild reaction conditions, good dispersion of nanoparticles, less chemical additives and non-poisonous by products; but, reaction rate is too slow. For the

synthesis of silver nanoparticles using bacteria, the time for completion of the reaction may range from 24 h to 120 h [11]. Microemulsion method is one of the best methods due to uniform and size controllable nanoparticle production; however, it is complicated to apply in industry and the process requires significant amount of solvent in purification system [12]. On the other hand, chemical reduction is foremost preferred technique among them for production of large quantities of nanoparticles in relatively short periods of time. Moreover, nanoparticles with different shapes can be easily prepared by controlling the reaction conditions. However, extraction of the nanoparticles in powder form may tend to either grow or aggregate leading to the large particles. As a result of aggregation, the nanoparticles may lose their properties. Thus, the most important key in this method is to avoid the agglomeration of silver particles during the synthesis and in the following preservation.

As mentioned above, there are three main components of the metal nanoparticle production systems: metal precursor, capping, and reducing agents.

Gold and silver, which are also known as noble metals, are the most widely investigated metal nanoparticles due to their chemical inertness, the tunability of their optical properties by controlling size, and their biologically mild side effects. Gold has a better chemical inertness, long term storage and structural robustness compared to silver. Although the reduction of silver ions is more difficult than gold,

silver salts are preferred in some cases due to their low cost and higher conductivity.

Silver salt precursors are generally used to produce ionic silver which can be reduced. Among silver salt precursors, silver nitrate is the most widely used one due to its low cost and chemical stability according to Tolaymat et al. [13].

The second component of the system is capping agents which are necessarily used for the prevention of particle agglomeration. They do not only inhibit agglomeration but also manipulate the shape and size of metal nanoparticles due to their chemical structure. Agglomeration is mainly caused by excess surface energy [14]. A stabilizing agent based on the repulsion forces caused by surface charge, steric stabilization, or both. Polymers which contain functional groups such as thiol (-SH), cyano (-CN), carboxyl (-COOH), and amino (-NH$_2$) attract the metal ions and stabilize them. Additionally, different types of surfactants and ligands can be used for this purpose. Although their usage may differ depending on the application area, citrates, amine and amides functional organics, polyvinyl pyrollidone (PVP) and cetyl trimethylammonium bromide (CTAB) are the most widely used capping agents [13]. In addition to the functional group of stabilizers, their chain length and concentration in solutions have significant effects on the shape and size of the particles. For example, Yamamoto et al. used carboxylic acids as stabilizing agent for silver particles, and showed that the decrease of the size of silver particles with the length

of carboxylate group [15]. When carboxylic acids with 7, 13 and 17 carbon were used, spherical silver particles with diameters of 15.4, 4.4, and 2.7 nm were produced, respectively. Additionally, the standard deviations of these particles are 5.1, 0.2 and 0.3, respectively. It indicated that the distribution of particles is also function of type and shape of the stabilizing agent [15].

Reducing agents may be the most important component of metal nanoparticle production systems, since they determine the number of seeds and the rate of the seed formation; and in turn the particles size and the shape of the nanocrystals. In a typical reduction mechanism, reducing agents reduce the metal ions and form seeds. These reduced particles can be used as seeds or nucleation centers for the growth of the particles. Capping agents inhibit or slow down the further growth and help to keep the particles at nano size. There are many reducing agents used to reduce silver salts.

The first study to prepare nanoparticles belongs to Turkevich et al. [4]. They used $HAuCl_4$ and trisodium citrate and produced gold nanoparticles with a diameter of approximately 20nm. Similar procedure using silver salts leading to the formation of larger particles. Nanoparticles were not uniform in size/shape and highly polydisperse due to few seeds formation and slow growth mechanism. So they obtained larger nanoparticles with a broad size distribution. By guidance of this study many reduction mechanisms have been developed in the literature and small size, monodisperse, stable silver

nanoparticles were obtained. Most widely used reducing agents includes $NaBH_4$, sodium citrate, N,N-Dimethyl formamide (DMF), PVP, ethylene glycol, ascorbic acid, microorganisms, hydrazine, aldehydes, hydrogen gas, sugars, and amines [13].

Chen et al classified metal nanoparticle preparation methods by the chemical reduction according to the reducing agents used; radiation reduction of silver ions, formation of silver colloids with strong and weak reducing agents [10]. Among them, radiation reactions are discussed earlier in this section. The other two types of reactions were studied in different ways in literature. Studies show that it is very difficult to obtain a narrow size distribution with a reducing agent because of the uncontrollable reaction resulting from the rapid reduction of particles. The weaker reducing agent, the more controllable and smaller particles are [1, 12,.16-17]. In addition to these studies, small size, monodispersed nanoparticles with controllable size and shape were also synthesized in this study. Besides, two different mechanisms with different reducing agents and systems were studied and compared in terms of particle size, applicability, and dispersion property. Hydrazine and oleylamine/oleic acid systems were studied as strong and weak reducing agent systems, respectively.

2.1.1 HYDRAZINE SYSTEM

Hydrazine is one of the strongest reducing agents for silver ions. To reduce the strong reduction action, reversed wormlike micelle with polymer shield system was suggested in this study.

Surfactants are a kind of capping agents which has both hydrophilic and hydrophobic groups. When surfactants are dissolved in water, hydrophobic head of the surfactant molecules will be repelled by water, whereas hydrophilic tails are directed towards the water molecules. As surfactant concentration increases in the solvent, hydrophobic tails come close together to minimize the free energy of the solution. Whenever concentration exceeds certain value, micelle structures form. This concentration is known as critical micelle concentration (CMC). Micelle structure is illustrated in Figure 2.1.
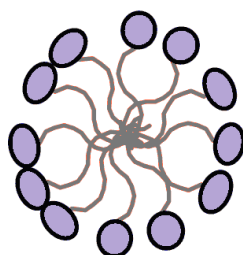
Figure 2.1 Micelle structure.

If the concentration of the surfactants continues to increase, micelle structures grow and depending on their tail structure (single chain, Gemini or trimetric) spherical, wormlike, and large lamellar micelles form (Figure 2.2).

11
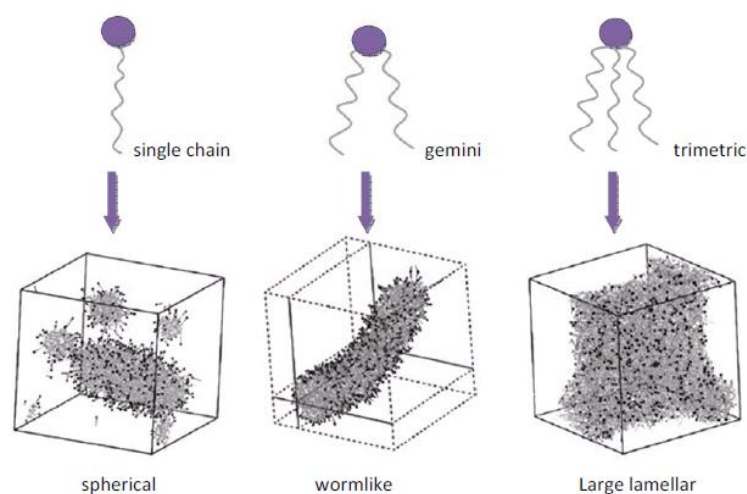
Figure 2.2 Types of micelles and their growth [18].

There are several types of surfactants; anionic, cationic, and nonionic. Ionic surfactants have tendency to attract counter ion. Therefore, when the counter ion is added into the solution, such as metal salts, ionic interactions become dominant over ion-water interactions in the system and micelle structure undergoes reversion. These types of structures are known as reverse micelle structures. In reverse micelle system, the free energy increases because of hydrophobic tails gathered in water. To stabilize the system a shielding polymer, which has tendency to interact both hydrophobic and hydrophilic structures, may be added such as polyvinyl alcohol (PVA). When hydrophilic polymers like PVA was added to the solution of reverse micelles, PVA shields the micelles and enhance their stability in water. The schematic representation of structure is given in Figure 2.3.
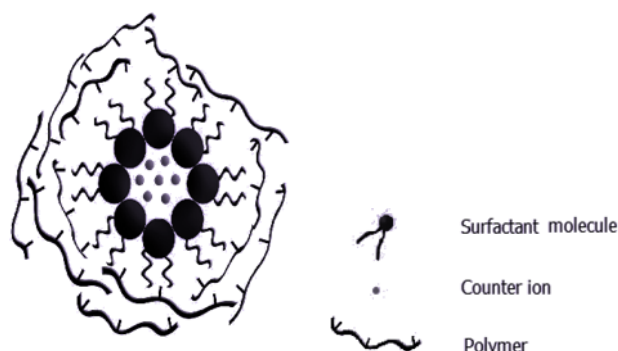
Figure 2.3 Reverse wormlike micelle shielded with hydrophilic polymer.

Gemini type surfactants have a pair of tails, and can pack very close with each other and form wormlike micelles. Dioctyl-sulfosuccinate sodium (DSS) is gemini type anionic surfactant and widely used for this purpose. It has considerably low CMC, which is 6.4×10^{-4}M [19]. Karakoc. built the model for Cu-DSS reverse micelle structure [20].

Sodium borohydrate [21], trisodium citrate [22], hydrazine [23] and hydroxylamine [24, 25] are examples of widely used strong reducing agents. In this study, hydrazine hydrate was also used as a continuation of Karakoc's work [20]. The dissociation reactions and solubility constants of hydrazine and its products were studied by Li et al [26]. According to Li et al.'s work:

$$N_2H_4 + H_2O \rightarrow N_2H_5^+ + OH^- \qquad K_b = 3\times10^{-6} \qquad (2.1)$$

$$N_2H_5^+ + H_2O \rightarrow N_2H_6^{+2} + OH^- \qquad K_b = 8.4\times10^{-16} \qquad (2.2)$$

$N_2H_5^+$ was assumed the only reaction due to low solubility constant, and total reduction mechanism of silver nitrate was given by Equation 2.3.

$$N_2H_4 \cdot H_2O + AgNO_3 \rightarrow N_2 + 4Ag + H_2O \tag{2.3}$$
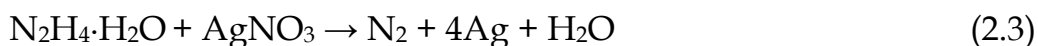
In reactions of silver and hydrazine hydrate ethanol was added to the solution to prevent oxidation, and decrease the rate of reactions. The reaction mechanisms related with ethanol was given by Equation 2.4 and 2.5.

$$AgNO_3 \rightarrow Ag^+ + NO_3^- \tag{2.4}$$

$$CH_3CH_2OH + Ag^+ + NO3^- + H_2O \leftrightarrow Ag(CH_3CH_2O) + H_2O + HNO_3 \tag{2.5}$$
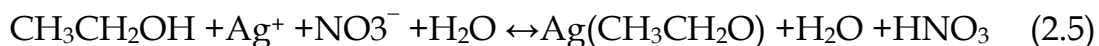
In the system, ethanol enhance the formation of $CH_3CH_2O^-$, ethoxy ion, therefore silver ions will be passivated for a while and strong reduction effect of hydrazine was reduced and oxidation of silver was prevented.

2.1.2 OLEYLAMINE/ OLEIC ACID SYSTEM

Oleylamine and oleic acid are used separately or together in many different systems. There is a wide range of studies in literature in

which oleylamine was used as a capping agent. Meanwhile, it was also used as a reducing agent in a number of studies. Actually, oleylamine should act both as a capping agent and reducing agent because of its long aliphatic tale and amine group, respectively. However, since it is a weak reducer, it serves as a capping agent in systems which contain stronger reducers than oleylamine or vice versa. For example, in the study of Deng et al., spherical silver particles with average diameter of 10 nm were produced at 150°C in the presence of oleylamine alone. However, as the Cu(I)Cl was added to the same system, in addition to the oleylamine, silver nanosheets were obtained after 24 h of reaction at 80°C without any disturbance [12]. Study of the Xu et al also gave an example of systems in which oleylamine was used as both reducing agent and stabilizer. The synthesize FeO particles from the oleic acid and oleylamine system with varying size between 14-100 nm which could be controlled by heating conditions. In this study, oleylamine was selected as alternative reducing agent and its excess amount enhanced the reduction reaction [27]. Same group also published the study about the reduction of Fe_3O_4 by only oleylamine. In this case, particles with diameter of 7-10 nm were produced as a result of one hour aging at 300°C. Another example about the multifunctional effect of oleylamine was the study of Mazumder et al. They concluded that oleylamine could be used as a solvent, surfactant and reducing agent for reducing the palladium ions; however, it cannot be used alone to synthesize monodisperse particles. This is due to longer reduction process leading to multinucleation and heterogeneous growth of nuclei. They

15

have also added borane tributylamine complex to the system as coreductant which is stronger than oleylamine [28]. According to these studies, it can be concluded that oleylamine has reducing effect on the metal particles, however, it is so weak that either broad particle size distribution is obtained or high temperatures are needed. Otherwise, it should be used with another reducing agent which is stronger than oleylamine.

Oleic acid is a good companion for oleylamine due to their chemical similarity. There are several studies in literature [2, 29-31] where oleylamine and oleic acid were used together for the stabilization and/or reduction of metal ions. However, to our knowledge, none of the studies explain the mechanism of the reduction and effects of the oleylamine and oleic acid in the system completely. In this study, their effects were also studied in detail and the mechanism was clarified.

2.2 ALIGNMENT OF METAL NANOPARTICLES

In addition to the size and dispersion of the produced nanoparticles, shapes of the particles also have great importance. Shape is one of the most important parameters to determine the properties of nanoparticles.

One dimensional structure have got great interest in recent years due to high surface area, colloidal stability, quantum conductance, low thermal conductivity, catalytic and antimicrobial properties, etc.

According to literature survey, there is no published result about the nanocable structure with silver cores. Only, the study of Song et al. is on the nanofibers made of oleylamine capped iron-platinum particles that are aligned in the core of PCL by coaxial electrospinning [32].

As mentioned before, nanowires are one of the most widely investigated structures as one dimensional metal structure. Tian et al produced silver nanowires with the diameter of 25nm and length of 20 μm from silver nitrate by using tannin ($C_{76}H_{52}O_{46}$) [9]. Wang et al produced oleylamine and oleic acid capped gold nanowires with the diameter of 2-9 nm and that are micrometer long [2]. Another study about the oleylamine capped silver nanowires belongs to Lu et al. The produced nanowires are 1.8 in diameter and length shorter than micrometers [33].

Comparing with nanowires, the advantage of nanocables is the possibility to obtain longer metal path inside the polymer sheath. In this study, the feasibility of this structure was demonstrated.

2.3 ELECTROSPINNING AND COAXIAL ELECTROSPINNING METHODS

There are several methods to produce nanofibers, namely phase separation [34], self assembly [35, 36], drawing [37], and

electrospinning [38-41]. Among these methods electrospinning is a simple, cost effective, convenient, and scalable technique for the production of continuous nanofibers. This process utilizes a high voltage DC source to inject charge of certain polarity into a polymer solution or melt. Polymer solution was drifted toward a collector of opposite polarity. As a result of the electrostatic attraction between the oppositely charged liquid and the collector, edge of the solution changes from rounded meniscus to a cone, called Taylor cone. When the electric field strength exceeded the surface tension of the liquid, a fiber jet is eventually ejected from the cone. While the fiber jet travels through the zone between the tip and the collector, the solvent evaporates and solid polymer fibers are deposited on the collector.

Electrospinning is the simplest route for preparing metal nanoparticle/polymer composites [42].

The examples in literature illustrate the feasibility of this approach. Copper nanoparticles generated by reducing $CuCl_2$ with hydrazine in solution in the presence of PVA yielded a suspension of elemental copper nanoparticles that was then electrospun into PVA/Cu nanoparticle composite nanofibers [43]. Jeon et al. studied polycaprolactone (PCL) based polyurethane (PU) nanofibers containing silver nanoparticles reduced in PCL/PU solution for use in antimicrobial nanofilter applications. They have annealed the nanofibers at 100°C for 24 hours to obtain monodisperse particles [44]. In another study, PVA nanofibers containing silver nanoparticles were

prepared by electrospinning PVA/silver nitrate aqueous solution, followed by short heat treatment and the residual silver ions was reduced by subsequent UV irradiation [45].

In this study, PVA shielded reverse micelle structure was used to prevent agglomeration and hydrazine hydrate was used to reduce silver ions in solution. Metal containing polymer composite was generated by single jet electrospinning without any heat treatment. According to literature, the produced composite nanofibers can be used in many areas due to unique properties of silver nanoparticles i.e. high catalytic activity, high electrical conductivity and antimicrobial activity, etc. [42-45].

Coaxial electrospinning is a modified version of electrospinning. In this technique two dissimilar materials can be prepared in core-sheath configuration. The only difference of coaxial electrospinning from the single jet is the capillary used. Coaxial electrospinning set up is illustrated in Figure 2.4.
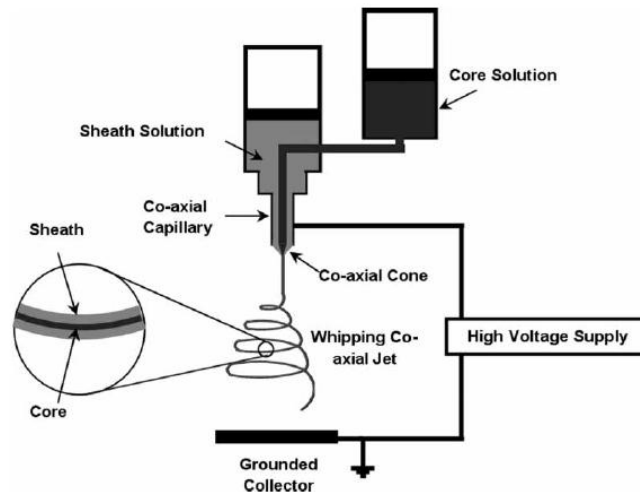
Figure 2.4 Coaxial electrospinning set up [46].

In this system, when the polymer solutions are charged using high voltage, charge accumulation occurs predominantly on the surface of the sheath liquid coming out of the outer coaxial capillary. The droplet of the sheath solution elongates and stretches due to charge-charge repulsion. Once the charge accumulation reaches a certain threshold value due to the increased applied potential, a fine jet extends from the cone. The stress generated in the sheath solution cause shearing of the core solution due to viscous dragging and contact friction [47]. This causes to accompany of core fluid to sheath solution and coaxial jet develops at the tip of the cones.
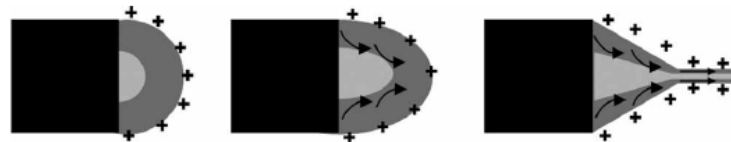
Figure 2.5 Taylor cone formation for coaxial electrospinning [46].

This technique gives a wide range of application area to such materials. For example, an unstable component can be isolated and the chance of decomposition under a highly reactive environment can be minimized. As other applications we can mention (i) release to a particular receptor with time, (ii) enhancement of mechanical properties of materials, and (iii) scaffolds for engineering tissues in which a less biocompatible polymer is surrounded by a more biocompatible material.

In literature, there are several studies to use coaxial electrospinning method for different applications. One of these approaches is to obtain fibers from non-electrospinnable materials. In these studies, sheath is used as a template or guide to the core material to form fibers even if the core material was not capable of forming fibers by itself in single jet electrospinning. To electrospun any solution, it should have moderate molecular weight, suitable molecular arrangement and viscoelastic properties. Therefore, sheath materials could be effectively electrospinnable for these studies.

One of the first studies with this approach belongs to Sun et al [48]. In their study, non-electrospinnable polymer poly(dodecylthiophene) and a metal salt palladium (II) diacetate was electrospun by dispersing them in a solution of PEO and ethanol-water as a core solution and pure PEO dissolved in ethanol-water as sheath polymer solution. The total diameter of fiber was about 3000 nm whereas the core diameter was about 2000 nm. This study demonstrated the feasibility of such

approach. Yu et al. studied PAN/PAN-co-PS and silk/PEO core/shell system and they showed the feasibility of the fiber production from the solution which is too dilute to spin. After they had removed the shell material in post treatment, they obtained fibers of core solution with the diameter of 100-200 nm [49]. In another study, PVP/PLA sheath/core system was produced to prepare biodegradable composite nanofibers structure for possible controlled particle release application like drug delivery [50]. The core/shell technique was also used by Li et al. [43]. They reduced $CuCl_2$ with hydrazine in solution in the presence of PVA and produced copper nanoparticles dispersed inside PVA fibers by coaxial electrospinning.

In the light of these studies, it seems possible to produce nanofibers with non-electrospinnable core. In this study, a metal nanoparticle containing polymer-free solution has been electrospun by the help of PCL shell. By this way, continuous metal core polymer shell nanocables have been produced.

2.4 PARTICLE SIZE ANALYSIS BY X-RAY DIFFRACTION

X-ray diffraction is very helpful to identify the crystalline structure, and the shapes of peaks contain additional and useful information. The width of a peak, for example, is a measure of the amplitude of thermal oscillations of the atoms at their regular lattice sites. Therefore, it is also a measure of imperfections in crystallite such as small particle size, strains and faulting. When crystallites are less than approximately

1000Å in size, appreciable broadening in the X-ray diffraction may also occur. Scherrer equation is a well known equation which explains peak broadening (Eq. 2.6). Once instrumental errors are excluded, the crystallite size can be easily calculated as a function of peak width, specified as the full width at half maximum peak intensity, full width half max (FWHM), peak position and wavelength.

$$< L >_{vol} = \frac{K\lambda}{B_{1/2} \cos\theta_B} \qquad (2.6)$$

In this equation, $< L >_{vol}$ is the volume weighted size, θ_B is the Bragg angle, λ is the wavelength of the X-ray and K is a unit cell geometry dependent constant whose value for silver particles is 0.89 [12], $B_{1/2}$ is FWHM of the peak after correcting for peak broadening which is caused by the diffractometer.

$B_{1/2}$ can be calculated as,

$$B_{1/2}^2 = B_{obs}^2 - B_m^2 \qquad (2.7)$$

where B_{obs} is the measured peak width and B_m is the peak broadening due to the machine. Peak broadening caused by the machine can be calculated by the estimation of FWHM value of almost perfect crystalline structure. The Peak Fit Software, which is used to analyze peaks and to get deconvoluted spectrum, is a good way to estimate

FWHM values.

2.5 SURFACE PLASMON RESONANCE

Surface plasmon resonance, SPR, is a widely used technique to characterize the optical properties of nanoparticles. In metal nanoparticles such as silver, the conduction band and valance band lie very close to each other in which electrons move freely. These free electrons give rise to a SPR absorption band, occurring due to the collective oscillation of electrons of nanoparticles in resonance with the light wave. The electric field of incoming wave induces a polarization of electrons with respect to much heavier ionic core of metal nanoparticles. As a result, a net charge difference occurs and this creates a dipolar oscillation of the all electrons within the same phase. Figure 2.5 shows the collective oscillation of the electrons, and it is called the dipole plasmon resonance of the particle. When the frequency of the electromagnetic field becomes resonant with the coherent electron motion, a strong absorption takes place, which is the origin of the observed colour.
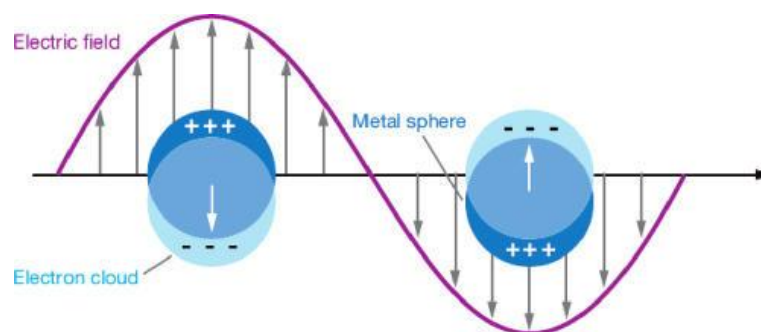
Figure 2.6 Schematic of plasmon oscillation for a sphere, showing the displacement of the conduction electron cloud relative to the nuclei [51].

24

The spectral position, FWHM and relative intensity of SPR depend on various physical parameters; dielectric functions of the metal and of the polymer, the particle size and shape distribution, the interfaces between the particles and the surrounding medium, the particle-particle interactions, and the distribution of particles inside the insulating material [5]. Therefore, SPR is a useful tool to characterize the optical properties of the particle and also particle size and shape. The shift in the SPR is related to changes in the shape of the nanoparticles and height of the SPR depends on the size of the particles. As particle size increases, absorption will increase for same concentrations. For different concentrations, FWHM value of absorption spectrum differs [52].

CHAPTER 3

EXPERIMENTAL

3.1 MATERIALS

The materials used in this study were tabulated in Appendix A.

3.2 EXPERIMENTAL PROCEDURE

Two separate systems were prepared to reduce silver nitrate to silver metal nanoparticles. In the first system strong reducing agent hydrazine hydrate was used. The prepared solution was directly electrospun with the aim of obtaining interconnected assemblies of the metal containing fibers. In the second case, a weak reducing agent, oleylamine/oleic system was used. The produced metal particles were then electrospun coaxially with a polymer to obtain nanocables.

3.2.1 HYDRAZINE HYDRATE SYSTEM

In this system, PVA, DSS, and water were used as a shielding polymer, surfactant, and solvent, respectively. Initially, 0.068M silver nitrate solution was prepared in 20 ml deionized water. Then, 0.0576mmol

DSS and 2.4 g PVA were added and the temperature was increased to 50 °C. After 4 hours of mixing, a homogeneous solution was obtained, and hydrazine hydrate was added to the solution at room temperature at a rate of 15ml/h. These initial parameters were adopted from the study of Karakoc [20]. Sodium bisulfide which had been used in order to prevent oxidation of metal particles in the study of Karakoc was substituted by ethanol due to in order to eliminate the precipitation of silverparticles. Ethanol was added to the system as co-solvent in order to slow down the reduction reaction and prevent oxidation of silver particles. Different concentrations were tested to adjust the amount of ethanol. The tested concentrations are given at Table 3.1.

Table 3.1 Ethanol/water ratio used.

H_2O (ml)	Ethanol (ml)	Ethanol/Total volume (v:v)
5	15	0.75
10	10	0.50
13	7	0.35
15	5	0.25

In order to fully understand the system, the effect of the amount of silver nitrate, the surfactant, and the polymer were studied as parameters in micelle formation step. The set of experiments conducted by different compositions are listed in Table 3.2.

Table 3.2 Set of experiments for micelle formation step.

AgNO$_3$ (M)	DSS (M)	PVA (%)
0.069	1.28	12
0.076	1.28	12
0.087	1.28	12
0.094	1.28	12
0.104	1.28	12
0.087	1.28	12
0.087	2.56	12
0.087	7.68	12
0.087	10.24	12
0.087	15.20	12
0.087	1.28	12
0.087	1.28	13
0.087	1.28	14

In addition, the reduction parameters of the system, such as hydrazine hydrate to silver ratio, and the hydrazine hydrate addition rate were optimized. The set of experiments are listed in Table 3.3. Hydrazine hydrate was introduced very slowly by means of a syringe pump.

XRD analysis was performed to check the complete reduction of silver nitrate to silver nanoparticles. To do that, a sample with appropriate amount of silver nitrate in ethanol-water solution was reduced by hydrazine hydrate solution. The product was separated by centrifugation, and was dried at 60°C. Then XRD pattern was

characterized. The details of XRD analysis was explained in following section.

Table 3.3 Set of experiments for the reduction step.

n_{HH}/n_{Ag^+}	HH addition rate (ml/h)
1.5	15
2.5	15
3.0	15
3.5	15
4.0	15
5.0	15
6.0	15
7.0	15
3.5	15
3.5	9
3.5	6
3.5	3

The parameters of electrospinning system had been optimized in the study of Karakoc [20]. It was observed that these parameters are also suitable for the silver system.

The electrospinning setup consists of a high voltage direct current (DC) supply, syringe pump, and collector. High voltage supply which has electrical potential range from 0 to 30kV is from GAMMA High Voltage Research Inc., USA (Model no: ES30P-20W/DAM) and the

multi-syringe pump is from New Era Pump Systems Inc. (Model no: NE-1600 Six-Syringe Pump). The syringe was 10ml in capacity with a syringe diameter of 16mm.

The positive electrode wire was attached to the metal body of the needle, whereas the negative part was connected to the metal collector. The metal collector was covered by aluminum foil and the setup was kept in a poly(methyl methacrylate) cage for safety considerations. The experiments were carried out at atmospheric pressure, and at room temperature. Figure 3.1 is a picture of electrospinning setup used in this study.
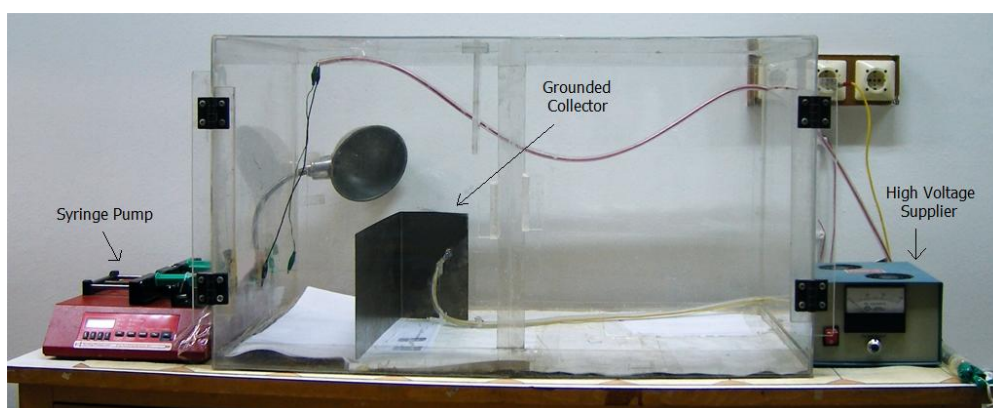

Figure 3.1 Electrospinning setup.

In the electrospinning experiments the previously optimized parameters such as flow rate 0.8ml/h, voltage 16kV, and with a tip to collector distance of 15cm.

XRD was used to analyze the metal particle formation, and SEM was used to observe the morphology of fibers. For SEM characterization,

samples were placed on carbon tape and coated with carbon. In this analysis, SEM of Zeiss Evo 50 was used. In order to differentiate metal and the polymer back scatter probe was used. Backscatter probes are used to detect the contrast between the zones with different chemical composition. High-energy electrons originating in the electron beam are reflected or back-scattered out of the specimen. Electrons scatter differently due to atomic weight difference of elements. Elements with high molecular weight backscatter the electrons stronger than light ones; therefore, they appear brighter in the micrographs. Due to considerable molecular weight difference between carbon and silver, the distribution and the size of silver particles can be observed by this probe.

3.2.2 OLEYLAMINE / OLEIC ACID SYSTEM

In this system, metal nanoparticles were synthesized first in hexane solvent and then the optimized solution was used as a core solution in coaxial electrospinning. The shell solution was prepared separately.

3.2.2.1 SILVER NANOPARTICLE SYNTHESIS

In order to synthesize metal nanoparticles, silver nitrate, oleylamine, oleic acid, and hexane were used. In the reaction, hexane was used as solvent whereas oleylamine and oleic acid were used as capping and reducing agents. Firstly, $AgNO_3$ was dissolved in the solution of oleylamine and hexane by sonication. Then, oleic acid was added into

the solution and mixed at high temperatures. After the completion of the reaction, the solution was cooled down to room temperature.

Table 3.4 Set of experiments for OAm/OAc system.

T (°C)	t (min)
80	120
115	120
150	120
115	50
115	120
115	270

Several set of experiments were conducted in order to understand the effect of each material in the mixture and the effect of parameters of the system. In these sets, the amounts of oleylamine, hexane, silver nitrate, and oleic acid were studied in addition to the reaction conditions, i.e. temperature and time. The set of experiments are listed in Table3.4 and 3.5.

The formation of metal particles was checked by X-Ray Diffractometer (RIGAKU D/Max-2200/PC) by using CuKα (λ=0.154nm) radiation at 40kV and 200mA. The structures of silver and other derivatives of silver in the system were estimated from the most intense peaks of phases. Additionally, the size of silver nanoparticles was determined from Scherrer equation by using FWHM value which is estimated by deconvolution of XRD patterns. The patterns were deconvoluted using

Peak Fit software (Peakfit, v. 4.11). An example calculation of particle size is given in Appendix B.

Table 3.5 Set of experiments for time and temperature parameters.

AgNO$_3$		OAc		OAm		Hexane
(M)	(mmol)	(M)	(mmol)	(M)	(mmol)	(ml)
0.168	2	0.5	6	0.0	0	10
0.126	2	0.4	6	0.8	12	10
0.101	2	0.3	6	1.2	24	10
0.092	2	0.3	6	1.4	30	10
0.084	2	0.3	6	1.5	36	10
0.170	2	0.5	6	2.6	30	0
0.101	2	0.0	0	1.5	30	10
0.288	6	0.1	3	1.4	30	10
0.184	4	0.3	6	1.4	30	10
0.169	4	0.5	12	1.3	30	10
0.235	6	0.7	18	1.2	30	10
0.088	2	0.4	9	1.3	30	10
0.039	1	0.7	18	1.2	30	10

To prepare samples for XRD, silver particles were separated from hexane, oleylamine, and oleic acid as much as possible by washing them with ethanol and by centrifugation. Samples were centrifuged twice at 10,000rpm at 20°C for 10min.

Additional particle size measurements of produced nanoparticles were done by dynamic light scattering technique using particle size

analyzer (Nanosizer ZS, Malvern Instruments Ltd.). Samples for this measurement were prepared by diluting the original solution ten times with hexane. Analysis was performed at 25°C and solution was kept at polystyrene cells during measurement. For each measurement six subsequent measurements were conducted and results were taken by using PCS analysis software. The results of the measurements were evaluated from cumulative volume data.

The morphology, size and distribution of particles were studied by using TEM (FEI, G2F30). Samples for this analysis were prepared by diluting the solution twenty times and drop casting on the carbon coated copper grid with 250mesh. Samples were dried at vacuum at room temperature before the analysis.

UV-Vis spectrum (Schimadzu, UV-2550) was used to characterize optical properties of metal nanoparticles. By this analysis, particle size and distribution were also studied. Sample solutions were diluted in appropriate proportions with hexane, and quartz cells were used in the measurements. Measurements were done in the range of 200-800nm of the spectrum.

3.2.2.2 COAXIAL ELECTROSPINNING

Several solutions were prepared for coaxial electrospinning. In all experiments the optimized silver solution was used, which includes

0.092M of silver nitrate, 1.4M of oleylamine, 0.3M of oleic acid and 10ml hexane, and it was prepared by mixing it at 115°C for 120min. Some of the experiments were conducted with direct electrospinning of the optimized solution, while the hexane content of the optimized solution was evaporated in some of them to increase the silver concentration at core. In order to enhance the electrospinning capability, dilute PVP in DMF solution was added to the optimized solution. DMF and hexane are insoluble in each other. To eliminate the phase separation in mixture and to increase the concentration of silvers in solution, hexane was evaporated as much as possible. In the shell part, PVP in DMF and PCL in TFE solutions were used because they are known with their high electrospinning capabilities. The combinations and compositions of these solutions are tabulated in Table3.6. In this table, the optimized solution and the hexane evaporated optimized solutions were shown by 'OS' and 'HEOS', respectively.

The setup of the coaxial electrospinning was same as the single jet electrospinning setup. The only difference was the spinneret consisting of two capillary tubes with one inside the other. A stainless steel capillary was used in this study with an exit orifice diameter of 1.1 and 2.5mm for inner and outer capillaries, respectively. The inner capillary tube acted as an electrode and connected to a high voltage source. Two separate syringe pumps were used in order to adjust the flow rates of the inner and the outer solutions independently.

The morphological characterization of cable structures was done by using SEM (Quanto 200F –Fei Field Emission Gun) in UNAM. In order to differentiate silver particles from polymer fibers backscatter detector of SEM was used. The samples were placed on double sided carbon tapes and micrographs were taken without any coating.

Table 3.6 Combinations and compositions of solutions for coaxial electrospinning.

Core Solution	Shell Solution	
Content	Content	Concentration
OS	PVP in DMF	20wt%
OS	PVP in DMF	30wt%
HEOS	PVP in DMF	20wt%
OS	PVP in DIW	20wt%
OS	PCL in TFE	8wt%
HEOS	PCL in TFE	8wt%
HE(OS+PVP in DMF)	PCL in TFE	8wt%

CHAPTER 4

RESULTS AND DISCUSSION

4.1 HYDRAZINE HYDRATE SYSTEM

In the study carried by Karakoc [20], copper salt had been capped with a surfactant polymer shield and copper ions had been reduced by hydrazine hydrate. $NaHSO_3$ had been added to the system to prevent oxidation of copper.

The preliminary experiment was a repetition of this abovementioned study with silver nitrate salt. However, it was seen that sodium bisulfide resulted in the precipitation of silver. In hydrazine hydrate reactions studied in the literature, ethanol was added to the system to prevent oxidation of silver particles and to slow down the reduction reactions of silver ions.

To adjust the amount of ethanol, four different volume fractions of ethanol between 0.25 and 0.75 were tested. The ratio of 0.75 was too high to dissolve PVA. For the ratios of 0.5, 0.35, and 0.25, the color of the solution was brown, grey, and dark grey, respectively. Brown is the color of silver in the oxidized form whereas grey is color of

metallic silver. Therefore, the ratio ethanol to total volume was taken to be 0.35.

In order to check and control the formation silver, samples were extracted from the solution of reduced silver nitrate and characterized by XRD. The patterns of the samples are shown in Figure 4.1.
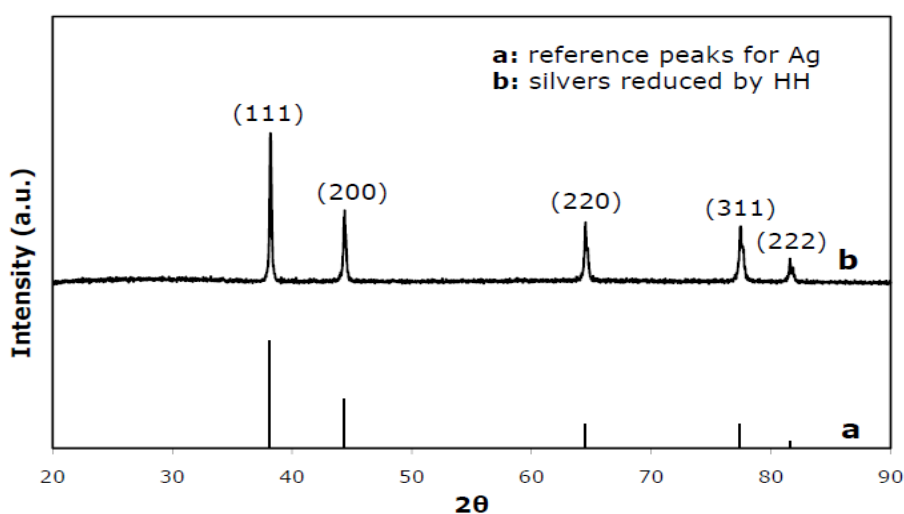

**Figure 4.1** XRD pattern of the sample produced by HH method.

The diffraction peaks at $2\theta=38.1$, 44.3, 64.5, 77.4, and 81.5° can be indexed as the (111), (200), (220), (311), and (222) planes of face centered cubic silver, respectively. The position and relative intensity of all diffraction peaks matched well with the standard peaks.

After this achievement, all parameters of the system were studied subsequently. For each of them, micelle formation, reduction, and electrospinning steps were studied and results were compared for

their fiber morphology, and the dispersion of silver particles in/on fibers.

The amount of silver was chosen as the first parameter studied for this system. To do that, five different compositions between 0.069 and 0.104M were used. It can be observed from the SEM micrographs in Figure 4.2 that at lower extreme of these compositions, there is very small amount of silver stationed in/on fibers. When the amount of silver was increased to an excess amount, particles became agglomerated. Then, the amount of silver nitrate was fixed as 0.087M.

(a)   (b)
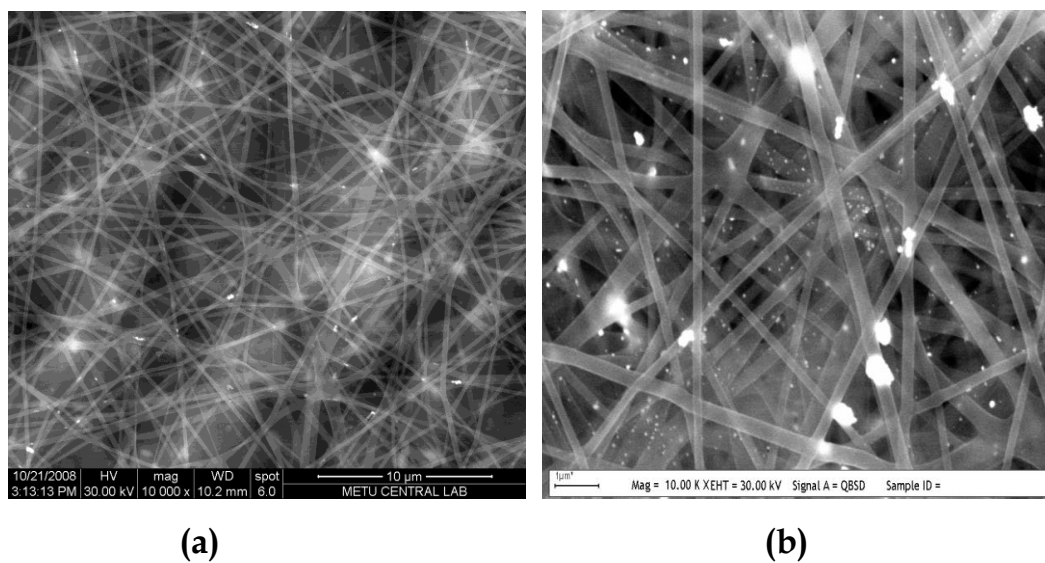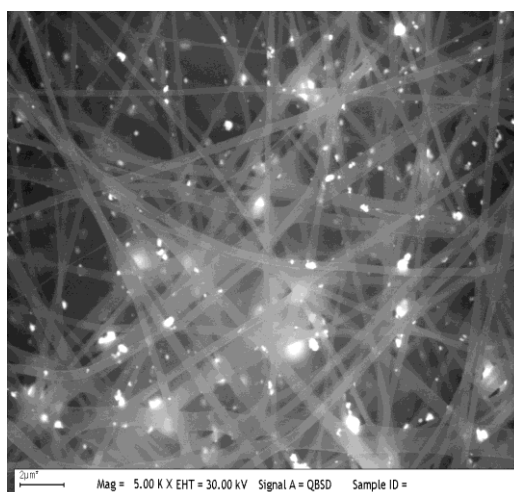
(c)

Figure 4.2 SEM micrographs of samples with different silver nitrate concentrations; (a) 0.069M, (b) 0.087M, (c) 0.104M.

Polymer and surfactant concentrations were important parameters for this system due to their effect on viscosity, and thus, effect on the electrospinning ability of the solution, fiber diameter, and morphology. However, they did not affect the silver particle distribution in fibers. Results of this parametric study are given in Appendix C.

As mentioned before, hydrazine hydrate is a strong reducing agent. The addition of ethanol, the use of surfactant, and shielding by polymer can slow down the fast reduction. However, these changes are not yet enough to obtain monodisperse metal particles in polymer fibers. The fast reduction can be slowed down by lowering the hydrazine hydrate to silver nitrate ratio (HH/$AgNO_3$), and also the addition rate of solution. Figure 4.3 and 4.4 are the SEM micrographs of fibers produced with these parameters.
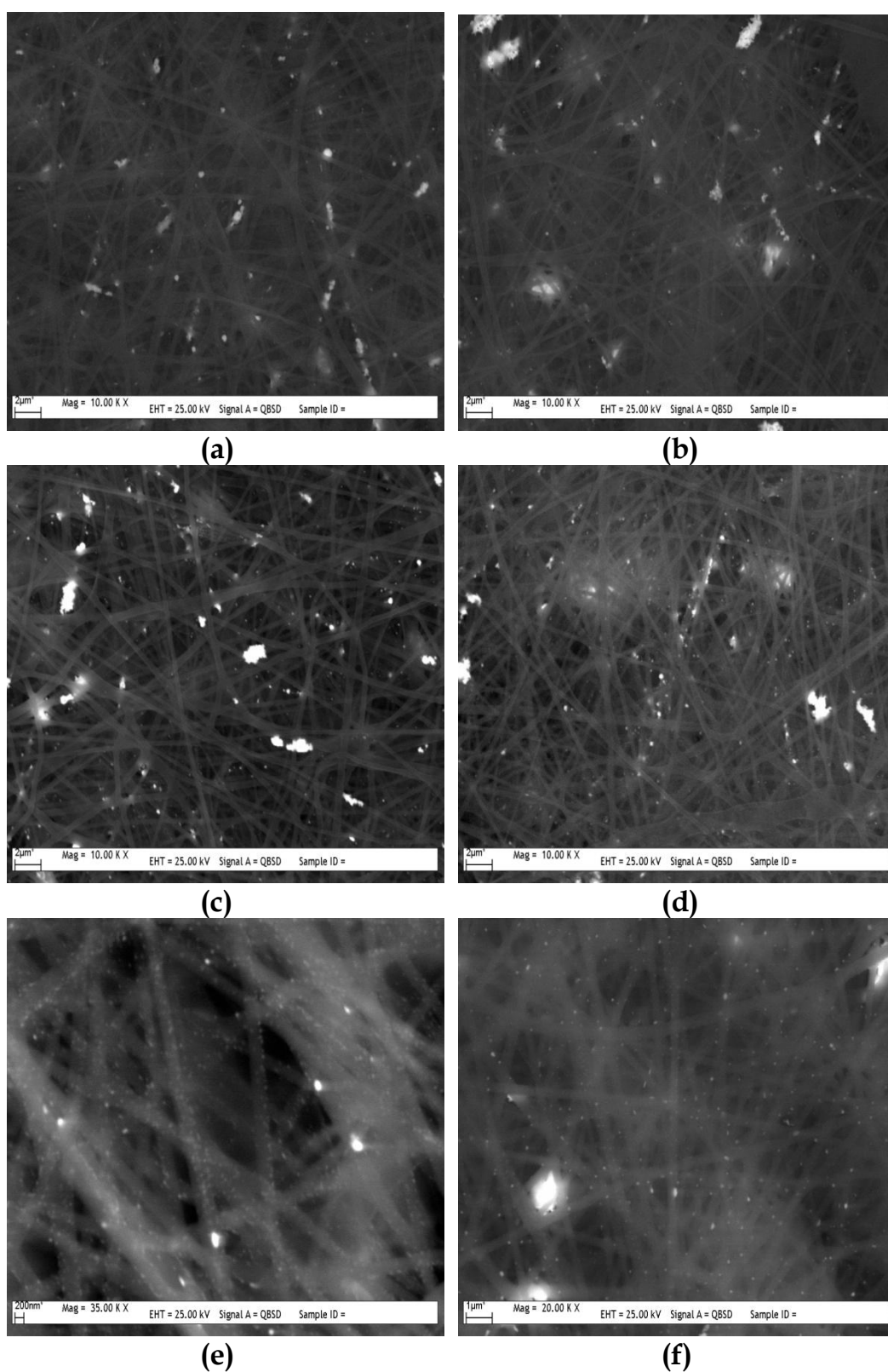
Figure 4.3 SEM micrographs for samples with different $HH/AgNO_3$ ratio; (a) 1.5, (b) 2.0, (c) 2.5, (d) 3.0, (e) 3.5, and (f) 4.0.

According to SEM micrographs in Figure 4.3, the increase in HH/AgNO₃ resulted in an increase in the number of smaller particles, preventing the formation of big clusters. Silver particles then started to station in fibers, and some kind of assembly was obtained especially for the ratios of 3.5 and 4.0. However, it could be achieved at a limited extend and there were still large clusters in samples. SEM micrographs for the ratio of hydrazine hydrate to silver nitrate ratio above the 4.0 are given at Appendix C. These samples did not any important difference or improvement in the results of these parameters.

The effect of the rate of addition was shown in Fig. 4.4. It is seen that even a very small addition rate (i.e. 3ml/hr) could not help to prevent the agglomeration of particles.

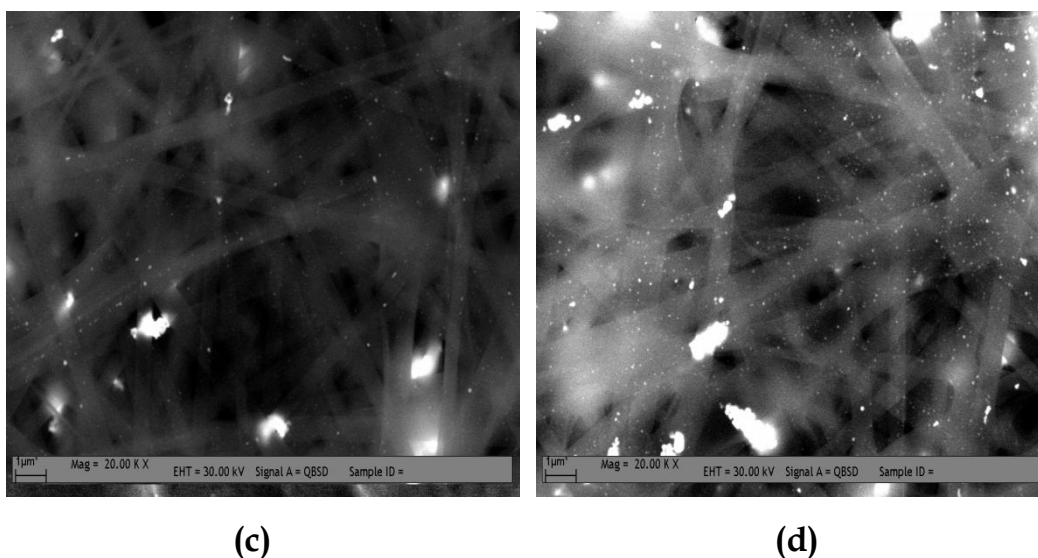(a)   (b)

(c)   **(d)**
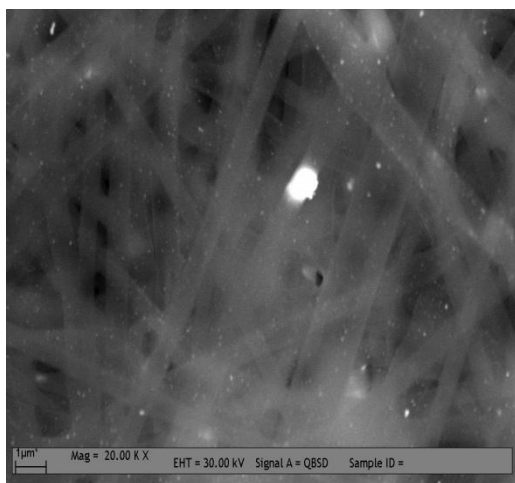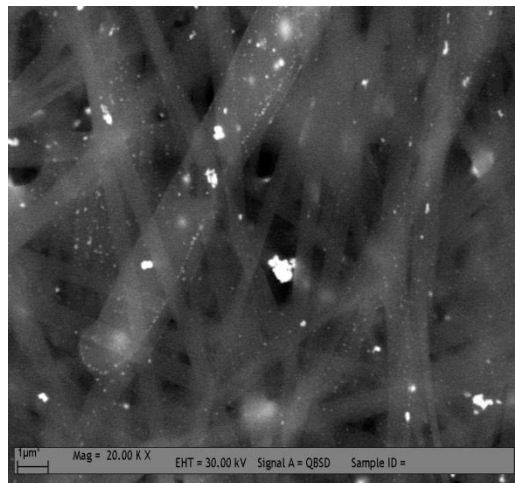
Figure 4.4 SEM micrographs for different hydrazine hydrate solution addition rates; (a) 15ml/h, (b) 9ml/h, (c) 6ml/h and (d) 3ml/h.

The aim of all these parameters studied about HH system was to decrease the strong reduction effect of hydrazine and to control the particle size and distribution. However, as seen in the SEM micrographs apparently, particle size distribution in fibers are too broad. It was obvious that no matter which capping agent is used or which operational parameters are changed, agglomeration of particles cannot be efficiently prevented and the distribution of the particle size are generally very broad.

To sum up, it is necessary to use of strong capping agents with weak reducing agents in order to control the particle size and the size distribution. To obtain aligned and interconnected particles, the control of the system is necessary by the use of slowly acting reducing agents. To demonstrate the feasibility of such a system,

oleylamine/oleic acid system was studied in which both components act as reducing and capping agents at the same time.

4.2 OLEYLAMINE/OLEIC ACID SYSTEM

In order to control the kinetics of reduction reaction, strong capping agents were used together with the weak reducing agents. Oleylamine and oleic acid are the chemicals which has functional group at the head of their aliphatic tales with 18carbon. These functional groups attack the metal ion and form a micelle. The aliphatic tails help to keep the micelles in suspension with aliphatic solvents. Oleylamine and oleic acid also act as reducing agents, reducing metal ions inside the micelle. In this way, particle formation is expected to be controllable.

First of all, typical particles obtained from OAm/OAc system were analyzed by XRD to characterize the formed structures. As shown in Figure 4.5, four peaks were observed belonging to diffraction from (111), (200), (220), and (311) planes of face centered cubic (fcc) silver, respectively. There are no other peaks in the pattern indicating the high purity and single phase. Additionally, all peaks are extremely broad since crystallites begin to lose their expected shape and imperfections in crystallites increase with decrease in size. The broadening becomes observable especially for the ones smaller than 1000Å. The occurrence of broadening in each plane, and the proportionality in diffraction intensities mean that particle size decreased from all directions and spherical particles were obtained.

Additionally, the observation of symmetric peaks in the diffraction patterns is an indication of uniform size distribution, i.e., formation of monodispersed particles. In addition to the information obtained from the XRD pattern, TEM and PCS analysis were performed for further characterization of the nanoparticles formed.
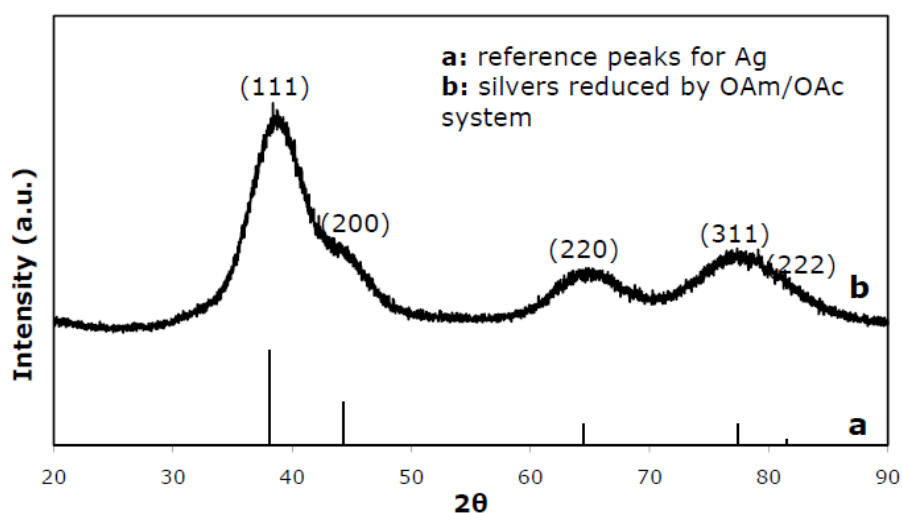

Figure 4.5 XRD pattern of typical solution.

Making sure that pure silver nanoparticles were produced, we proceeded with the particle size analysis. The best technique to analyze nanoparticles is TEM. By this method, both structural and morphological analysis can be done; however, it was relatively expensive method and it was not so accessible. On the other hand, XRD and PCS can be used complementarily for the analysis of nanoparticles. Although these methods are common and easy to use, their outputs should be analyzed very carefully. It is because they are not based on direct observation, but some indirect derivations. In order to obtain some correlation between the methods, three samples prepared in different conditions were analyzed in detail.
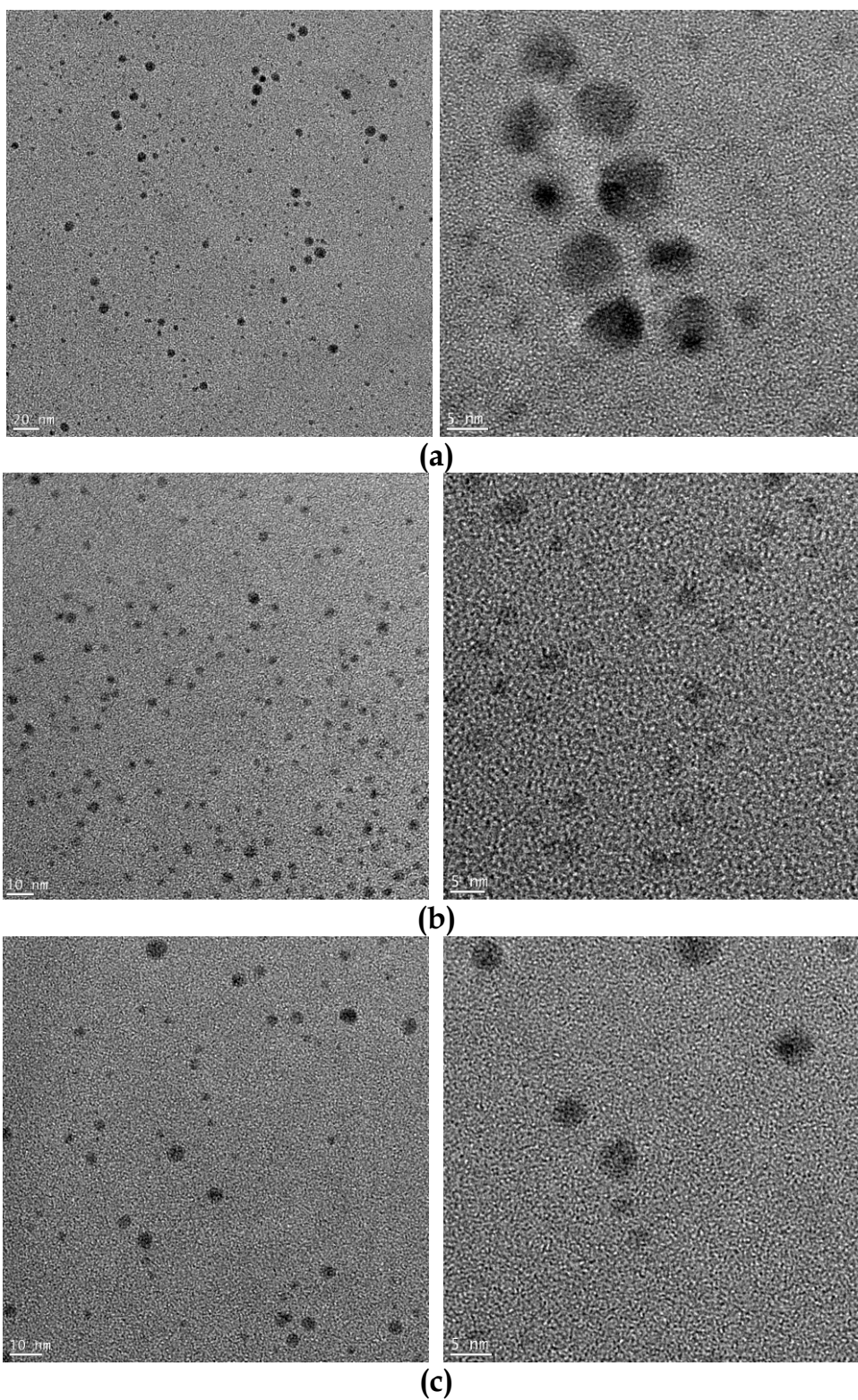
Figure 4.6 TEM micrographs for typical solution of metal nanoparticles (a) at 115°C, (b) at 150°C, and (c) sonificated but magnetic stirring was not used.

It is shown in Figure 4.6 that particles were distributed almost homogeneously in the solutions and no agglomeration was observed. Particle sizes measured from these figures were listed in Table 4.1 for comparison.
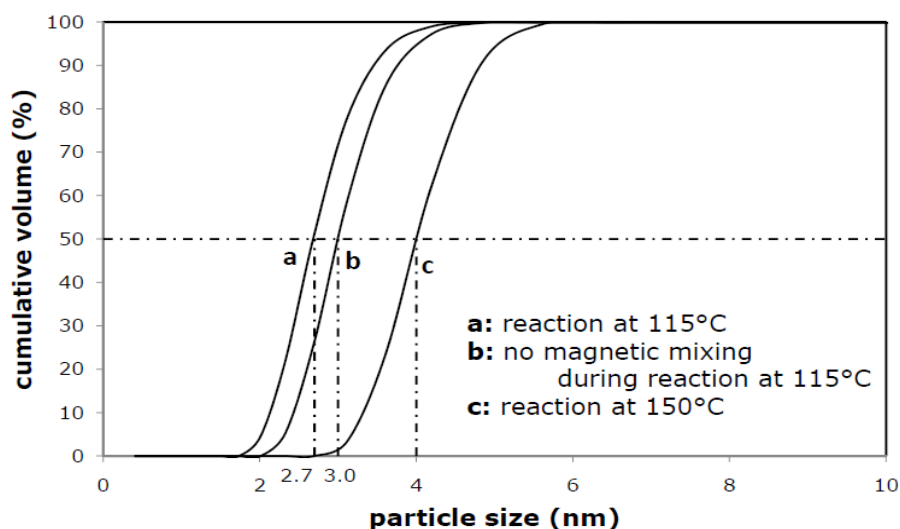

Figure 4.7 Volume weight average particle size calculations from PCS data.

The size and size distributions of selected samples obtained from the PCS analysis are shown in Figure 4.7. From this data, it can be concluded again that there is no agglomeration in the system, and particles are distributed almost monodisperse. Particle size calculations from XRD data by Scherrer Equation are explained in Appendix B. For comparison, the average particle sizes are tabulated in Table 4.1.

Table 4.1 Particle sizes calculated from different characterization methods.

Sample	TEM (nm)	PCS (nm) (volume-weight average)	XRD (nm) (Scherrer eqn)
115°C	2.8±1.9	2.7	1.5
150°C	3.8±1.3	4.0	1.7
Sonication but no mixing	2.8±1.3	3.0	2.0

As shown in Table 4.1, TEM and PCS results are very close to each other. However, the results obtained from XRD data are a bit different from others. When TEM micrographs at higher magnifications are analyzed, it is seen that there are two phases (i.e. metal & polymer) in particles. Additionally, the length of oleylamine which is between two nanowires was measured between 1 and 2nm in literature [33]. Therefore, it can be concluded that XRD results are measures of real crystallites which can be seen from TEM micrographs at higher magnifications, whereas TEM and PCS measure the OAm and OAc capped silver particles. According to these results, particle size and size distribution measurements were then made by PCS.

After the correlation study, the parameters of the system, the type of mixing, time, temperature, the amounts of oleylamine, oleic acid and silver nitrate were analyzed.

Firstly, the effects of mixing were studied and the particle size and size distributions are given in Figure 4.8. When the solution was not well

mixed (a), two apparent phases occurred in the system indicating the incomplete reduction and some of the silver ions remained in the solution. In the case that sonication was used to disperse silver particles in oleylamine and hexane solution, but left the solution without mixing during the reaction (c), particle size distribution was not more different than the solution mixed by both sonication and magnetic stirrer (b); however particles were smaller in the case of 'b' as expected. Due to smaller particle size, both sonication and magnetic stirring were used in the experiments.
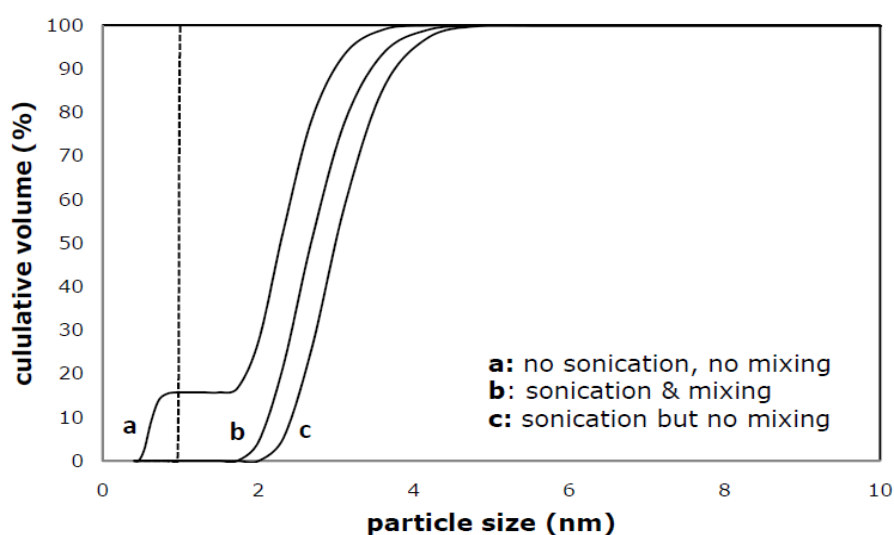
Figure 4.8 Effect of mixing.

The effect of reaction time on particle size and size distribution is shown in Figure 4.9. It was observed that color did not change during the reaction lasting for 50mins. It means that the silver particles did not form. The color of the solution began to change from yellow to brown after one hour. Then, color turned into dark brown. The 4.5h of

duration was too long, and particles grew bigger with broad size distribution. Finally, reaction time was fixed to 2hrs.
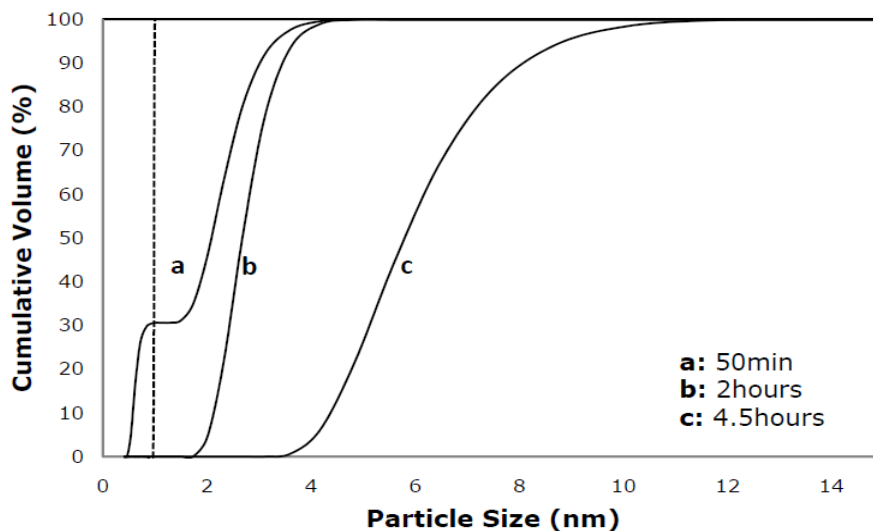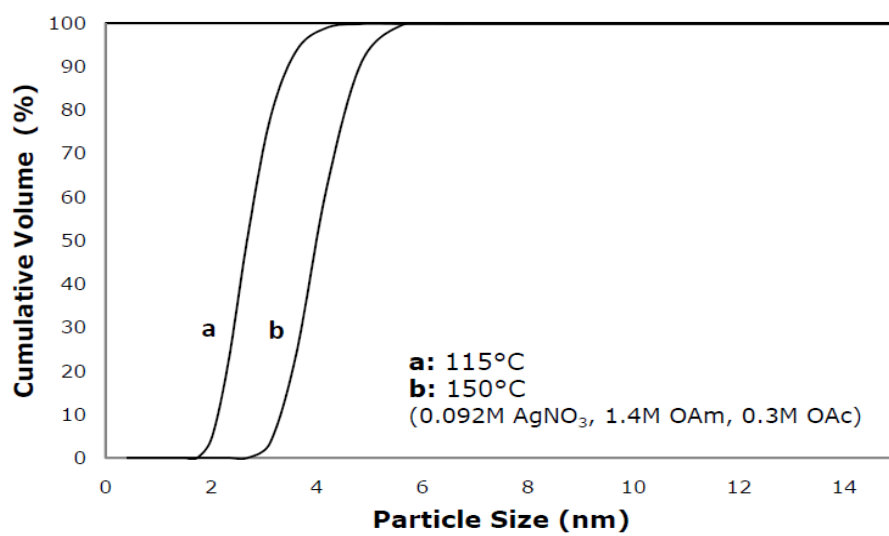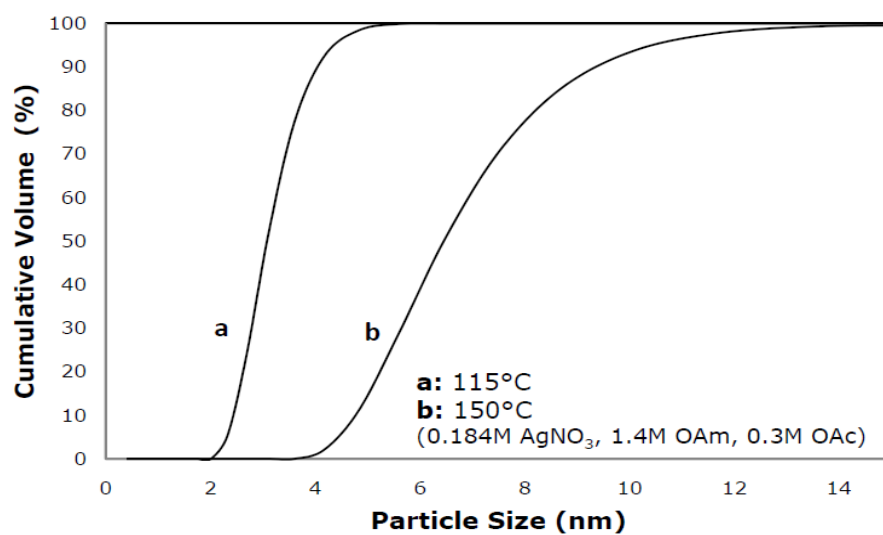

Figure 4.9 The effect of reaction time.

When the temperature effect was studied for different concentrations, it was observed that increasing temperature results in increasing in particle size and broadening in the size distribution as seen in Figure 4.10 as expected. Independent on the concentration, particles grew faster at high temperatures due to increase in their kinetic energy. Below 115 °C, silver particles were not produced as observed from the color of the solution. Therefore, temperature was fixed to 115 °C during reaction. According to temperature effect results, it can be said that weak reducing agents need higher temperatures than strong ones to complete reduction and this allows the control of the particle size. Temperature differences affect the growth of particles slightly; therefore, particle size can be tuned by adjusting temperature.
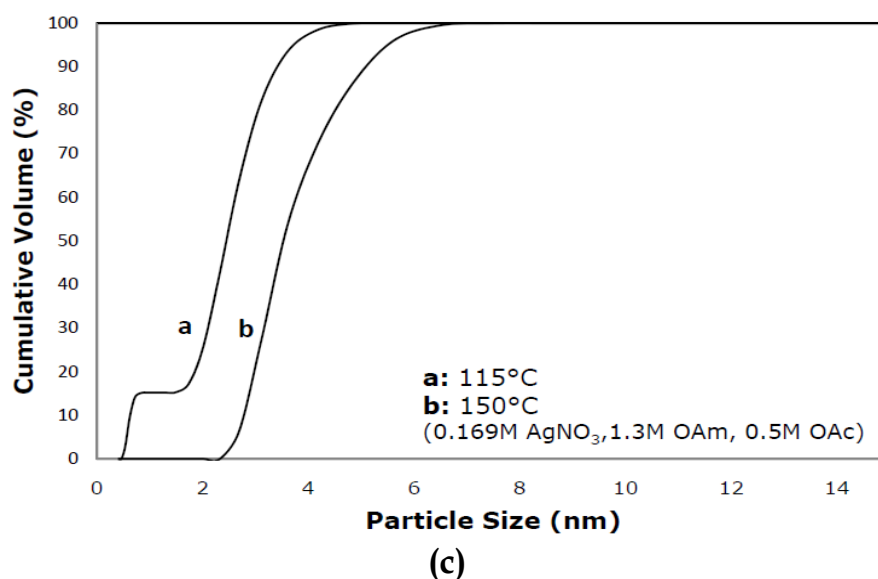
(a)

(b)

51

Figure 4.10 Effect of temperature for different concentrations.

After optimizing the reaction conditions, the effect of each component on the reaction was studied. In the first step, silver nitrate was dissolved in oleylamine and hexane solution by sonication. In the absence of hexane or oleylamine, silver nitrate cannot be dissolved or distributed in the solution, indicating that hexane and oleylamine have the function of a solvent. Hexane has aliphatic structure and without any functional groups. Therefore, hexane should carry the oleylamine and enhance its stability in the system as a solvent. On the other hand, amine groups of oleylamine are expected to have an interaction with the metal ions. The effect of oleylamine was examined by several sets of experiments with different oleylamine concentrations keeping the other parameters constant. In these experiments, 0.3M oleic acid was added to the solution of 10ml hexane and appropriate amount of oleylamine in which 0.092M silver nitrate dispersed by sonication. Figure 4.11 shows the PCS results of these sets.
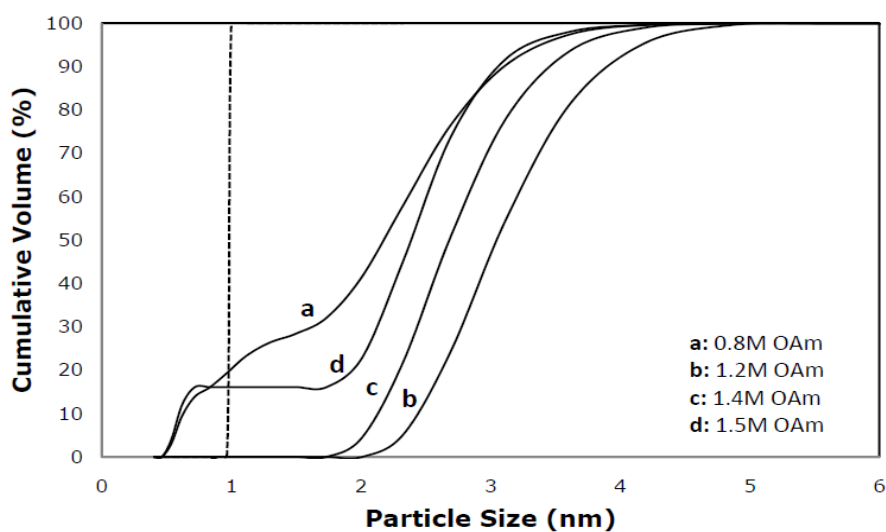
52

Figure 4.11 Effect of oleylamine with different concentrations on particle size and size distribution of silver.

As shown in the figure, oleylamine has some effect on the particle size distribution of silver particles. Oleylamine was not sufficient to get fine distribution of particles for the concentration of 0.8M. In the case of 'd' where OAm was 1.5M, some of the particles did not have a chance to grow because of the excess amount of OAm. Additionally, these smaller particles stayed out of the detection range of the device which shown by dashed line in the figure, and below that the results lose their reliability. On the other hand, samples with 1.2M and 1.4M OAm seem better, and 1.4M case has narrower distribution than 1.2M OAm case. Therefore, in the subsequent experiments 1.2M OAm was used. According to these results, especially due to the difference between first and last concentrations, it can be said that oleylamine improves the poor solubility of silver nitrate in hexane. Due to interaction between oleylamine and silver ions, some of the dissolved silver nitrate molecules were removed from hexane through capping.

Therefore, the dissolution of silver nitrate in hexane would be increased.

In the absence of oleic acid the color of the solution remains yellow and does not return into dark brown which indicates the formation of metallic silver particles. That means oleic acid serves as reducing agent in the system. Otherwise, two hours of reaction time is not enough for oleylamine to reduce the metal ions alone. To get better understanding of the mechanism, the amounts of oleic acid and silver nitrate were changed, and a series of experiments were conducted.

Figure 4.12 shows that the increase in the quantity of silver nitrate leads to the growth of particles, and thus to broader distribution as expected because, as the concentration of silver ions increases, the amount of oleylamine per silver ion would decrease and more ions would be capped by the same amount of oleylamine. If silver particles were abundant, capping could not be much effective, and the distribution comes out to be broad. In the case of 'a', the concentration of silver did not change as much as in case 'b' and an increase in particle size was observable from the figure. On the other hand, in case 'b', broadening in distribution of particle size became more significant. Therefore, it can be concluded that the dispersion of particles can be tuned by adjusting the concentrations of the components.
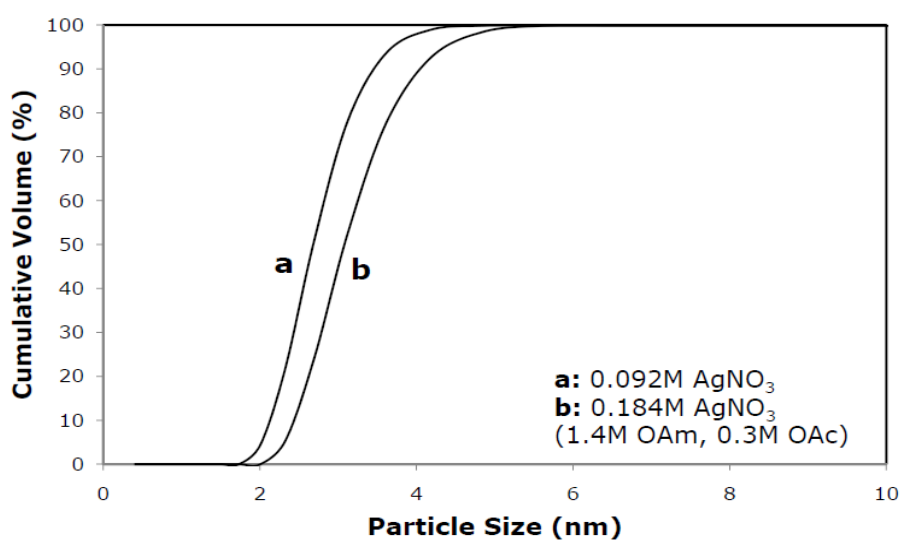
(a)
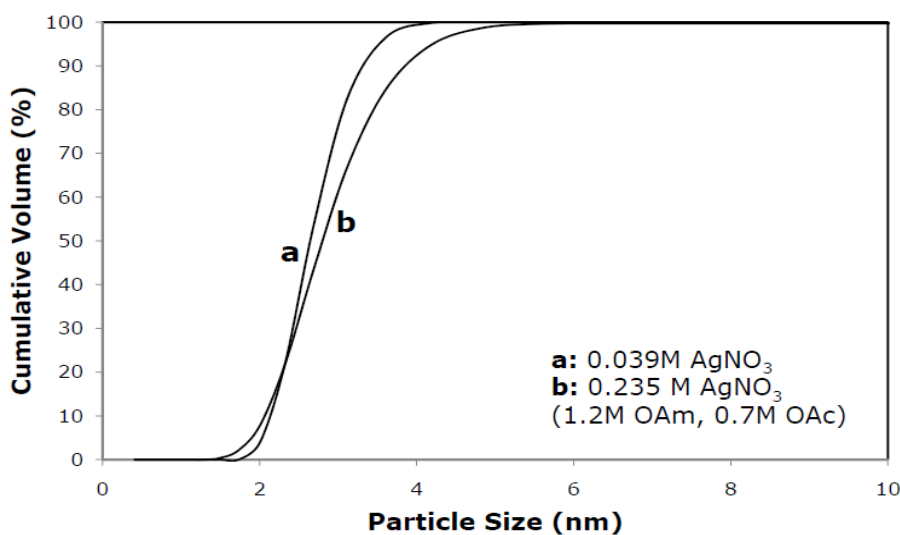
(b)

Figure 4.12 The effect of the quantity of silver nitrate at different
concentrations.

Figure 4.13 shows the effect of oleic acid amount in the system. In case
of 'a', 0.3M oleic acid was not enough to complete reduction of 4mmol
silver nitrate in solution or time was not adequate to obtain
monodisperse growth of particles with that amount of oleic acid. On
the other hand, once the concentration increased to 0.5M, silver ions

were reduced completely and particles distributed well. In case 'b', amount of silver nitrate was low and the difference in particle size and size distribution was not significant. Decrease in oleic acid amount resulted in bigger particles since reduction was completed in a relatively large time interval and particles grew much. Actually, oleic acid enhances the dissolution of silver nitrate into silver and nitrate ions as a result of interaction between silver ion and carboxyl group of oleic acid. Then, dissolved silver ions are easily attracted by amine groups of oleylamine and reduced. Therefore, as oleic acid amount decreases, silver ions interact with carboxyl groups less and there will be limited initiation points for the reduction. Since reaction continues from these points, fewer in number but larger silver particles will be formed.
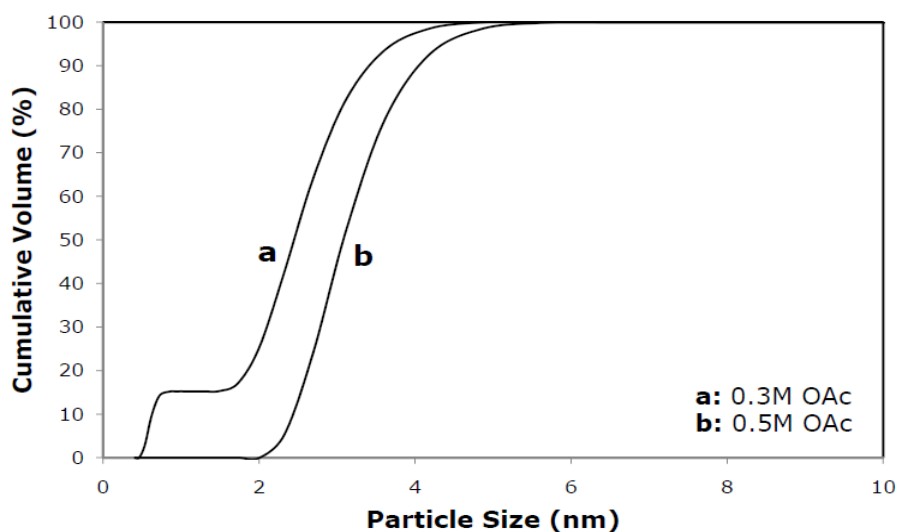
(a)
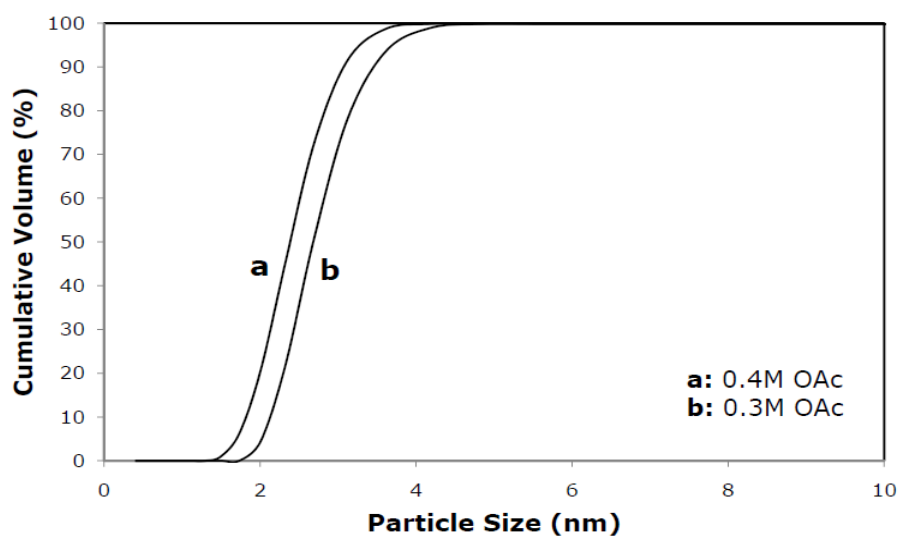
(b)

Figure 4.13 The effects of OAc concentrations for different concentrations; (a) 4mmol AgNO$_3$ and 30mmol OAm, (b) 2mmol AgNO$_3$ and 30mmol OAm.

As a result of this parametric study, the procedure for the preparation could be summarized as follows:

1. Mix the hexane and oleylamine,
2. dissolve silver nitrate in the solution by sonication,
3. add oleic acid to the solution,
4. raise the temperature to 115°C,
5. agitate the solution by a magnetic stirrer for 2hrs.

Compositions of silver nitrate, oleylamine, and oleic acid in the final solution were 0.092M, 1.4M, and 0.3M, respectively. Particle size and size distribution of the optimized solution was shown in Figure 4.14. This solution was described as the optimized solution and used in the nanocable production experiments. However, it is clear that particle

size and size distribution can be controlled by changing the composition or/and the parameters of the system.
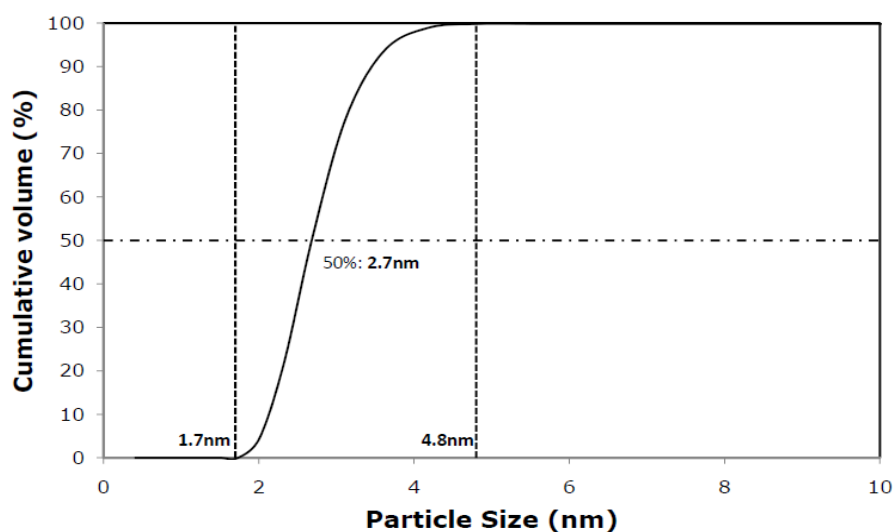

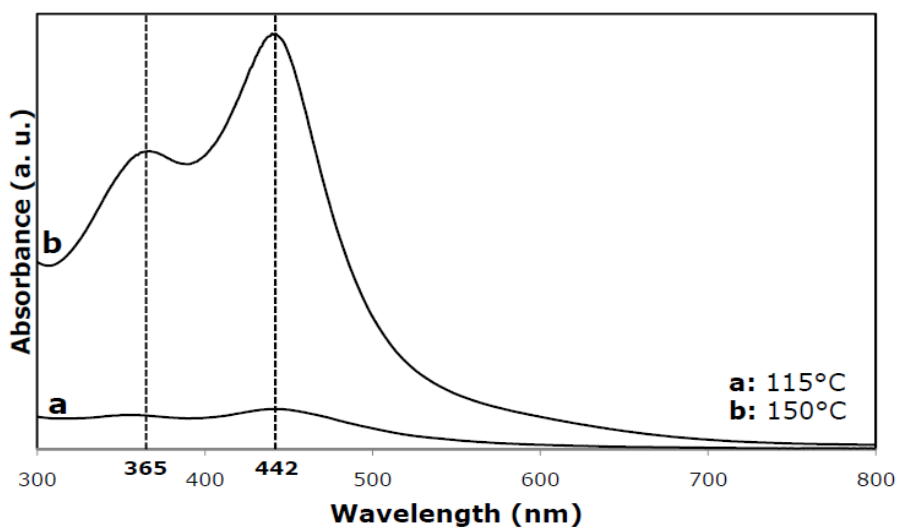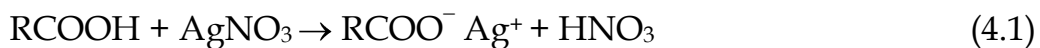**Figure 4.14** Particle size and size distribution of the optimized solution.

Figure 4.15 The changes in UV-vis spectra of samples prepared at different reaction temperatures with 12.5times dilution; (a) 115°C, (b)150°C.

SPR analysis was also conducted in order to characterize the optical properties of the particles. These results were also used to observe the particle size and distribution. Figure 4.15 shows the UV-vis spectra of the samples prepared at 115 and 150°C under the same concentrations.

It can be said that particles produced had high optical density due to their sharp absorption peaks. Moreover, the expected SPR absorption peak for silver particles is between 400-450nm. The lower wavelengths in SPR spectra represent the smaller particles in the solution. Two peaks in the spectra show two types of particles with two different particle sizes. However, if such data are compared with the cumulative volume particle size data from PCS, there are extremely small silver particles in the solution. But, the quantity of smaller particles is so little that it can be neglected. Additionally, the changes in the absorption intensity indicated the increase in the particle size which was observed by PCS analysis. It is clear that SPR results are also comparable with PCS and TEM data.

According to this study, it can be concluded that OAm and OAc reduced the ions by a common action. Firstly, amine groups of oleylamine attract silver nitrate and enhance its dissolution in hexane by encapsulation. Then, oleic acid was added into the solution. Nitrate groups of silver nitrate leave from silver ions due to competition between nitrate and carboxyl groups (Equation 4.1) Therefore, amine groups of oleylamine are able to attract the silver ions and make a complex with them. Therefore, required potential for reduction was

decreased. The mechanism of complex formation was shown by Equation 4.2 and 4.3.

$$RCOOH + AgNO_3 \rightarrow RCOO^- Ag^+ + HNO_3 \qquad (4.1)$$

$$Ag^+ + e^- \rightarrow Ag \qquad E^\circ{}_{red} = 0.799V \qquad (4.2)$$

$$Ag(NH_3)_2{}^+ + e^- \rightarrow Ag + 2NH_3 \qquad E^\circ{}_{red} = 0.373V \qquad (4.3)$$

Reduction potentials of silver ion and silver ammine nitrate complex were obtained from the literature. Therefore, it can be said that even the exact values of reduction potentials are not same in oleylamine/oleic system, they were close to given values and OAm makes complex with silver and nitrate ions. By this way, rate of the reduction reaction is slowed down and almost monodisperse particles can be synthesized.

The complex formation was demonstrated by XRD results for the samples in which the reaction was expected not to complete like samples of '50 min' and 'sonication but no mixing'. The XRD results are given in Figure 4.16.
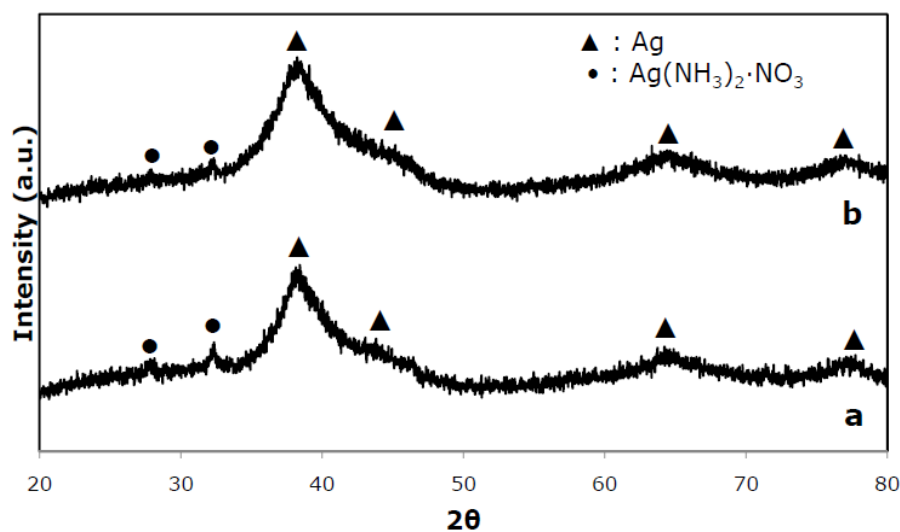
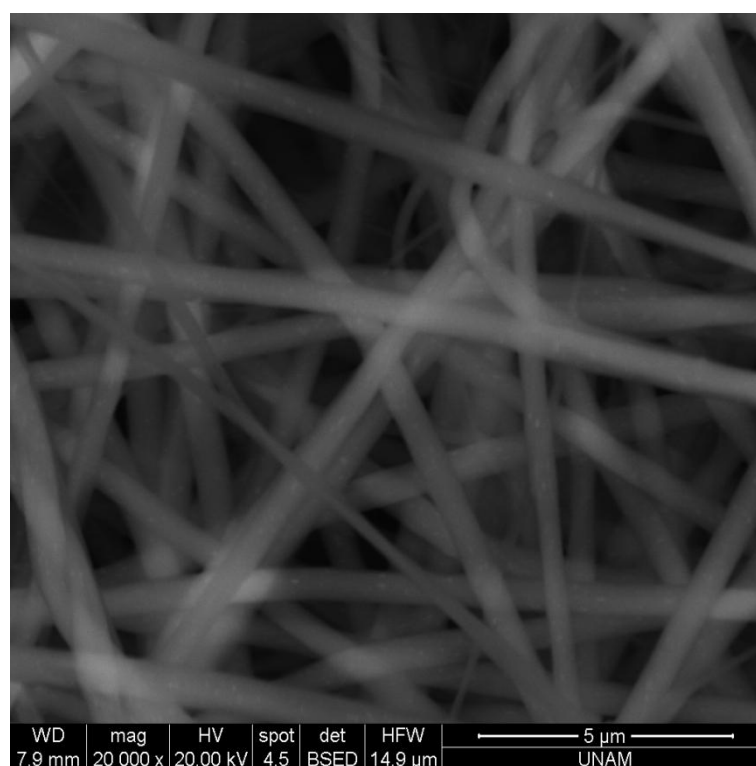**Figure 4.16** XRD patterns of 50min (a) and sonication but no mixing (b).

As shown Figure 4.16, peaks labeled by dots were impurities of silver production system. These peaks are the most intense peaks of the silver amine nitrate complexes in these 2θ values. These complexes were only seen in these solutions which are indicating an incomplete reaction. For 50min reaction time, it was expected less complete reaction and that can be observed from the data where intensities of the pattern were relatively higher than the ones of (b).

In this reaction, hexane serves only a solvent and OAm enhances the dissolution of silver particles in hexane by capping the ions.

4.3 COAXIAL ELECTROSPINNING

Optimized solution of OAm and OAc capped silver ions was used as core solution of the system. To electrospin this optimized solution, PVP in DMF or PCL in TFE solutions, which are known with their

high capability of electrospinning, were used. The parameters of the electrospinning system were adjusted according to the observation of the Taylor cone formation at the coaxial capillary tip. As a first experiment, the optimized solution was directly electrospun with shell solution of PVP in DMF. The SEM micrograph belonging to this example was shown in Figure 4.17. It is seen that silver particles were distributed on fibers and silver particles were not interconnected.
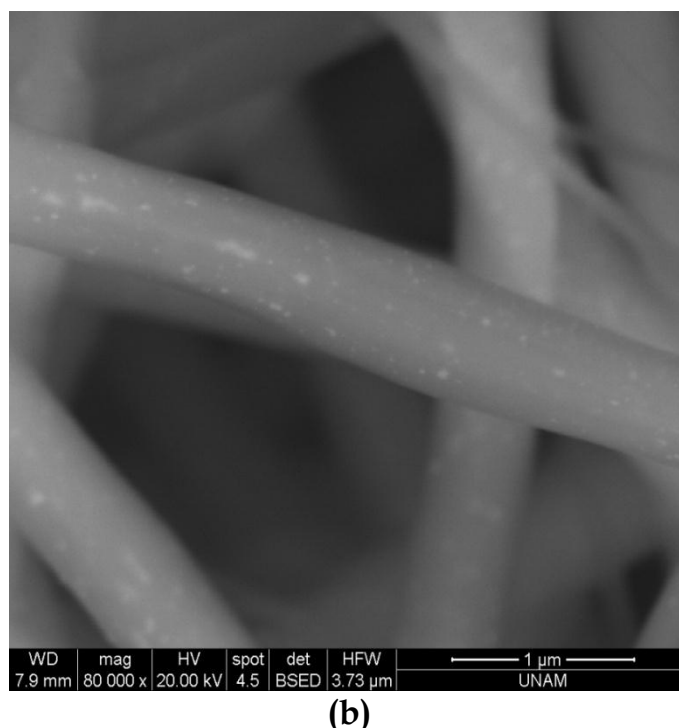

| WD | mag | HV | spot | det | HFW | 5 μm |
| 7.9 mm | 20 000 x | 20.00 kV | 4.5 | BSED | 14.9 μm | UNAM |

(a)

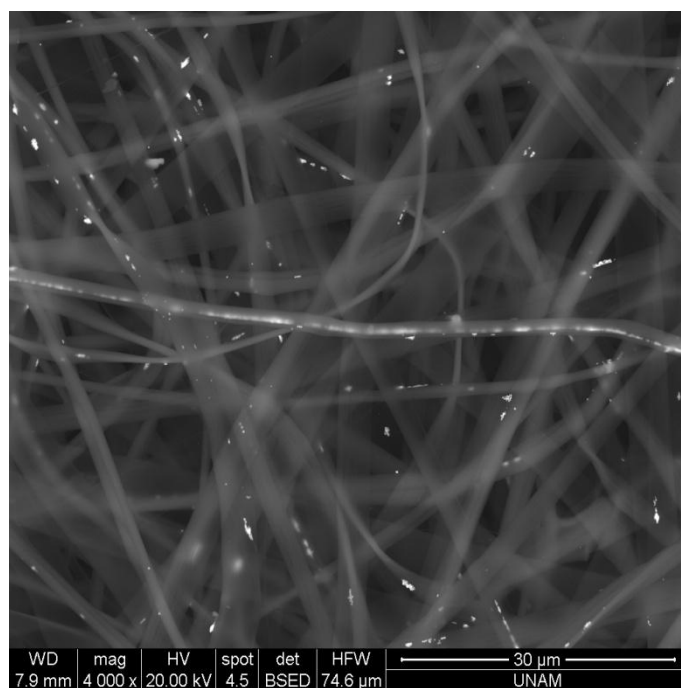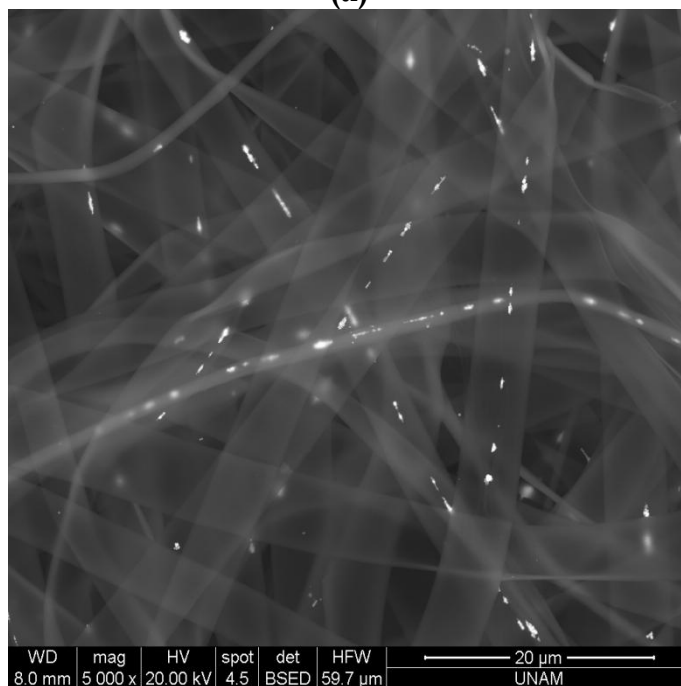| WD	mag	HV	spot	det	HFW
7.9 mm	80 000 x	20.00 kV	4.5	BSED	3.73 μm

1 μm — UNAM

(b)

Figure 4.17 SEM micrograph for the fibers with core of OS and shell of 20wt% PVP in DMF solution; (a) and (b) are micrographs at different magnifications

(ES conditions: flow rates (inner and outer solutions: 0.1, and 0.4ml/h; tip to collector distance: 14cm; voltage: 15kV).

It was thought that if the silver concentration in the core solution were increased, interconnection between particles might be obtained. For that reason, hexane content of the optimized solution was tried to be evaporated and this concentrated solution was used as a core solution. As shell solution 20wt% PVP in DMF was used. The SEM micrographs of the electrospun fibers are given in Figure 4.18. In these micrographs, it can be observed that silver particles gathered together and started to form interconnections. However, they are not yet well distributed in fibers.

WD	mag	HV	spot	det	HFW	30 μm
7.9 mm	4 000 x	20.00 kV	4.5	BSED	74.6 μm	UNAM

(a)

WD	mag	HV	spot	det	HFW	20 μm
8.0 mm	5 000 x	20.00 kV	4.5	BSED	59.7 μm	UNAM

(b)

Figure 4.18 SEM micrographs for core of HEOS and shell of 20wt% PVP in DMF solution; (a) and (b) are graphs belonging different parts of the same sample. (ES conditions: flow rates (inner and outer solutions: 0.4, and 2ml/h; tip to collector distance: 14cm; voltage: 17kV).

PVP in DMF is good but not the best polymer solution for electrospinning, because, it was difficult to adjust the parameters of electrospinning. For example, when the flow rate of a core solution was increased, the flow rate of a shell solution should also be increased accordingly. However, it turned out that, fibers became too thick and either Taylor cone could not easily form or it was not stable. Therefore fibers could not be produced or dried. To overcome this difficulty, the concentration of PVP in DMF solution was increased to 30wt% to increase the carrying capability. However, this solution was extremely viscous to electrospin. An improvement was attempted by substituting DMF with deionized water since it has lower boiling point. However, it did not work either. Finally, the shell solution was changed with PCL in TFE which is a solution easier to electrospin due to high polarity of components. For core of OS and shell of 8wt%PCL in TFE solution, two different conditions were tried. Figure 4.19 and 4.20 show the SEM micrographs of fibers obtained from these experiments. As shown in the figures, metal particles were aligned in polymer fibers. However, this could be achieved to a limited extend.
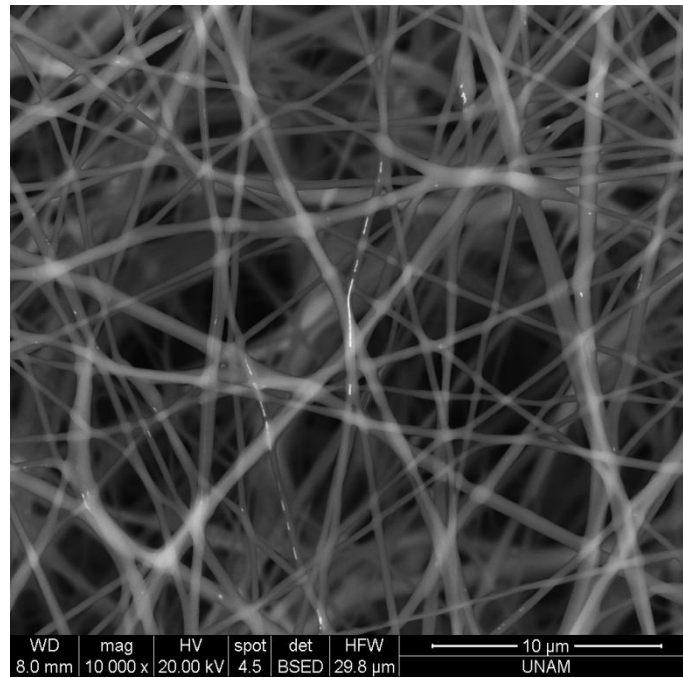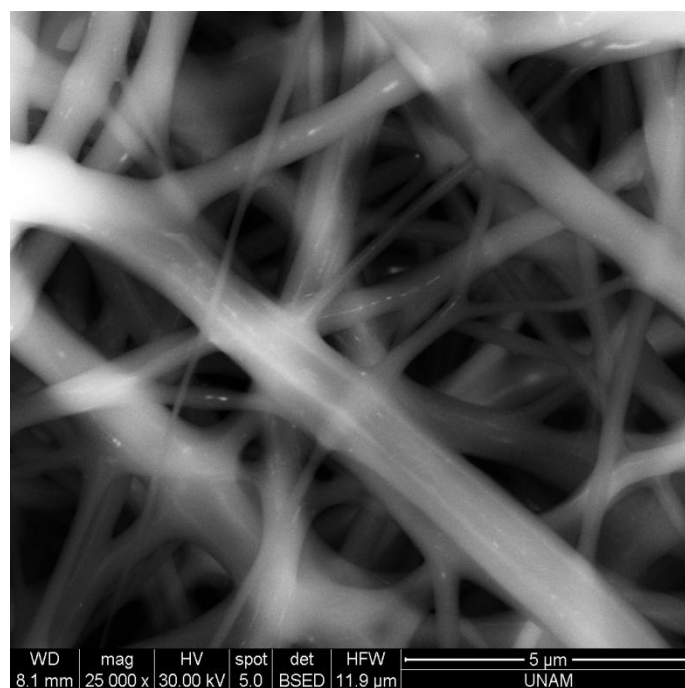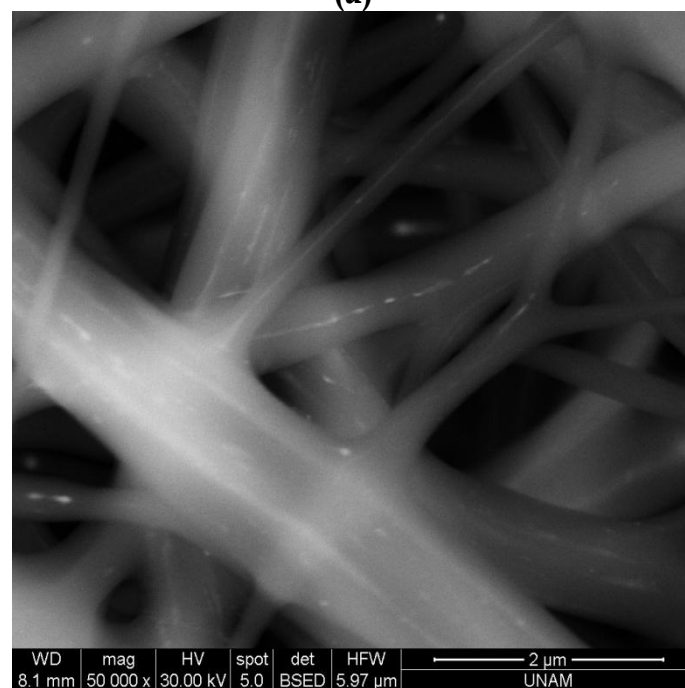
(a)
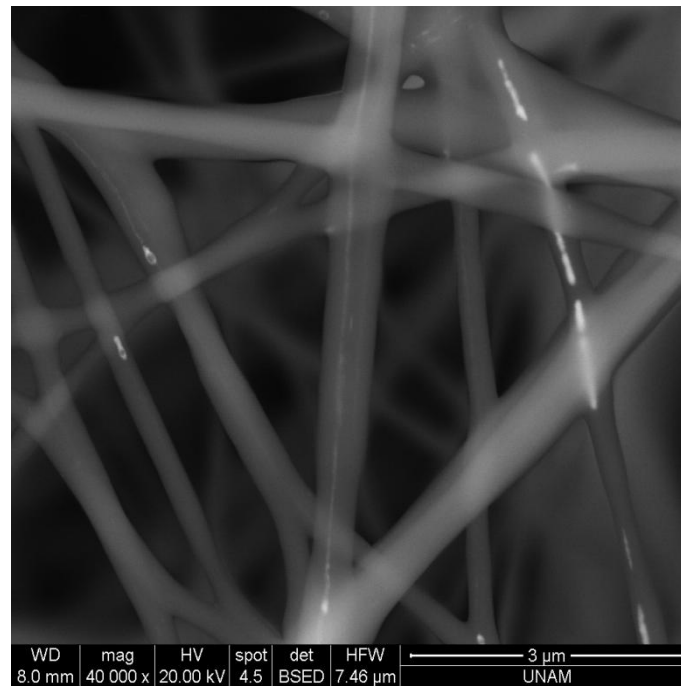
(b)

Figure 4.19 SEM micrographs for core of OS and shell of PCL in TFE solution with different electrospinning parameters at different magnifications (a) ×10000, (b) ×40000. (ES conditions: flow rates (inner and outer solutions): 0.1, and 0.4ml/h; tip to collector distance: 14cm; voltage: 15kV)

| WD | mag | HV | spot | det | HFW | 5 µm |
| 8.1 mm | 25 000 x | 30.00 kV | 5.0 | BSED | 11.9 µm | UNAM |

(a)

| WD | mag | HV | spot | det | HFW | 2 µm |
| 8.1 mm | 50 000 x | 30.00 kV | 5.0 | BSED | 5.97 µm | UNAM |

(b)

Figure 4.20 SEM micrographs for core of OS and shell of PCL in TFE solution with different electrospinning parameters at different magnifications (a) ×10000, (b) ×40000. (ES conditions: flow rates (inner and outer solutions): 0.3, and 1ml/h; tip to collector distance: 20cm; voltage: 24kV).

In order to improve the alignment of the metal particles and increase the concentration of the metal particles in the core, evaporation of hexane present in the core solution was tried for the samples with PCL shell. As shown in Figure 4.21, the silver particles in the core aligned continuously inside the PCL sheath. The diameters of the metal cores seem uniform in all cases.


| WD | mag | HV | spot | det | HFW | 4 μm |
| 8.0 mm | 30 000 x | 30.00 kV | 5.0 | BSED | 9.95 μm | UNAM |
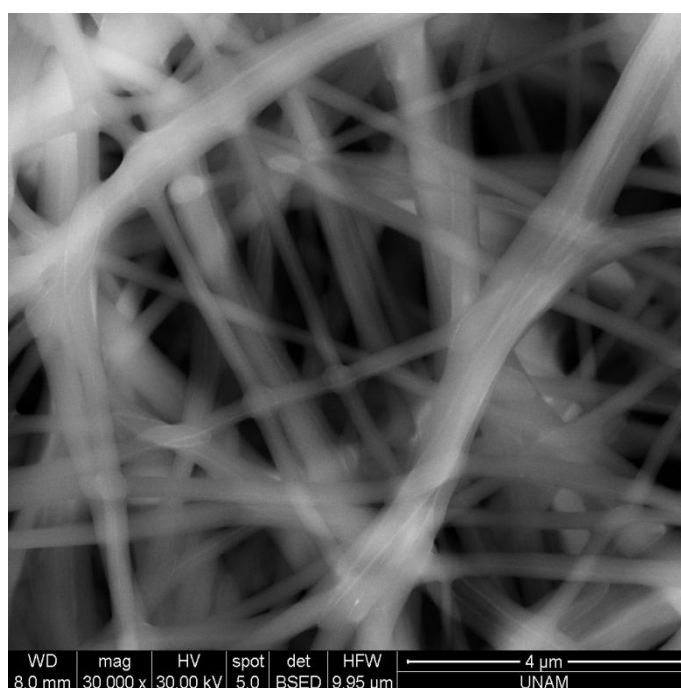
(a)
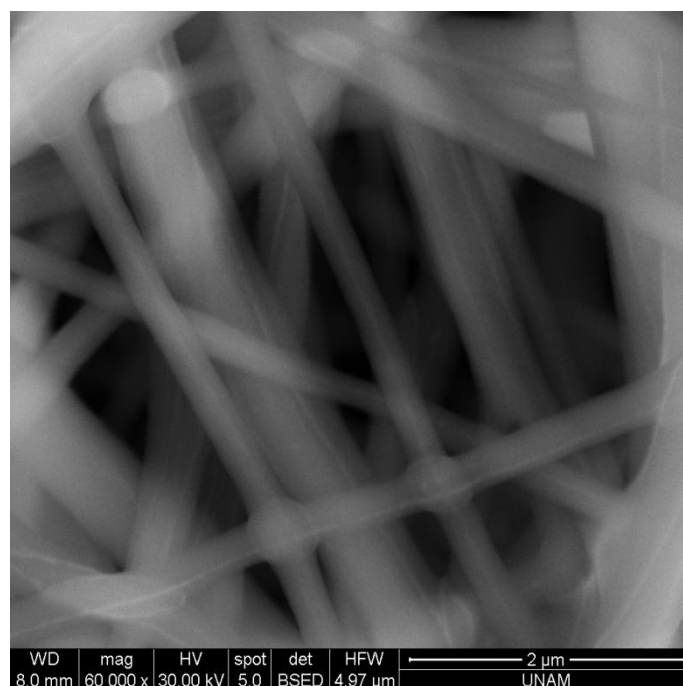
(b)

Figure 4.21 SEM micrographs for core of HEOS and shell of PCL in
TFE solution with different electrospinning parameters
(ES conditions: flow rates (inner and outer solutions: 0.4,
and 1ml/h; tip to collector distance: 18cm; voltage: 16kV).

It can be observed form the micrographs that cable structures are
formed successfully. Moreover, these cable structures could be seen in
all fibers in the micrographs.

A final improvement was done at the core solution for PCL in DMF
system. To enhance the electrospinning capability of the solution,
small amount PVP in DMF solution, 5wt%, was added into optimized
solution. Since hexane and DMF do not dissolve in each other, hexane
was evaporated from the solution. The produced fibers were also in
cable structure and their lengths are below 10µm as shown in Figure
4.22.
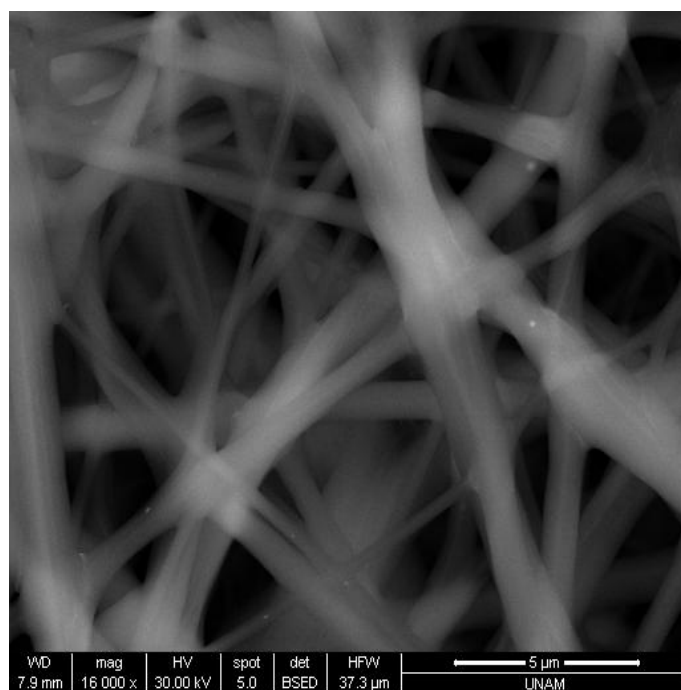
(a)
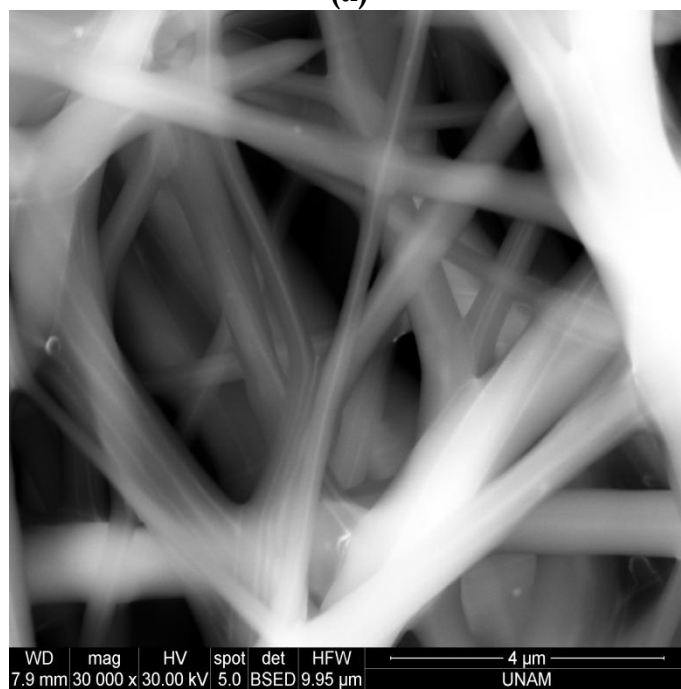
(b)

Figure 4.22 SEM micrographs for the fibers obtained from the HE
(OS+5wt% PVP in DMF) core and 8wt% PCL in TFE shell
solutions

(ES conditions: flow rates (inner and outer solutions): 0.1, and 1.5ml/h;
tip to collector distance: 16cm; voltage: 17kV).

70

CHAPTER 5
CONCLUSIONS

1. Independent of the capping agent, it is very difficult to control size and size distribution of particles below 20-30nm with strong reducing agents like hydrazine hydrate.

2. Oleylamine/Oleic acid system is a simple, versatile system to produce monodispersed metal nanoparticles with controllable sizes below 10nm.

3. Production of silver nanoparticles with precise size and size distribution can be achieved through the use of OAm/OAc system. Silver nanoparticles with sizes between 1.7 and 4.8nm and volume-weighted average of 2.7 nm were produced.

4. Coaxial electrospinning method was successfully used to produce fibers from solutions which are too dilute to electrospin or impossible to electrospin.

5. Synthesized metal nanoparticles are properly aligned in the core of the continuous polymeric fibers produced by coaxial electrospinning.

CHAPTER 6

RECOMMENDATIONS

1. Particles produced by oleylamine/oleic acid system can be characterized in detail. Therefore, new application areas can be found. For example, conductivity of such small metal particles may be extremely high due to quantum conduction.

2. According to the application area, cables produced in this work could be improved. For example, produced nanocables may be heat treated. As a result of decomposition of the polymer, pure aligned metal fibers may be formed.

3. Parameter adjustment and the control of the solution content prior to electrospinning will result in production of cables with better morphology and mechanical properties.

4. Decrease in the diameter of coaxial capillary leads to production of thinner cables.

REFERENCES

1. Wiley, B., Y. Sun, B. Mayers, and Y. Xia, "Shape-Controlled Synthesis of Metal Nanostructures: The Case of Silver," *Chemistry - A European Journal*, 2005. **11**(2): p. 454-463.

2. Wang, C., Y. Hu, C.M. Lieber, and S. Sun, "Ultrathin Au Nanowires and Their Transport Properties," *Journal of the American Chemical Society*, 2008. **130**(28): p. 8902-8903.

3. Cademartiri, L. and G.A. Ozin, "Ultrathin Nanowires - A Materials Chemistry Perspective," *Advanced Materials*, 2009. **21**(9): p. 1013-1020.

4. Challa, S. and S.R. Kumar, eds. *Metallic Nanoparticles*. 1 ed. Nanomaterials for the Life Sciences, ed. S. Challa and S.R. Kumar. Vol. 1. 2009, Wiley-VCH: LA. 571.

5. Carotenuto, G., L. Nicolais, B. Martorana, and P. Perlo, *Metal-Polymer Nanocomposite Synthesis: Novel ex-situ and in situ Approaches*, in *Metal-Polymer Nanocomposites*, G.C. Luigi Nicolais, Editor. 2004. p. 155-181.

6. Salavati-Niasari, M., Z. Fereshteh, and F. Davar, "Synthesis of oleylamine capped copper nanocrystals via thermal reduction of a new precursor," *Polyhedron*, 2009. **28**(1): p. 126-130.

7. Yu, W., H. Xie, L. Chen, Y. Li, and C. Zhang, "Synthesis and Characterization of Monodispersed Copper Colloids in Polar Solvents," *Nanoscale Research Letters*, 2009. **4**: p. 465-470.

8. Kim, S.-G., N. Hagura, F. Iskandar, and K. Okuyama, "Characterization of silica-coated Ag nanoparticles synthesized

using a water-soluble nanoparticle micelle," *Advanced Powder Technology*, 2009. **20**(1): p. 94-100.

9.   Tian, X., J. Li, and S. Pan, "Facile synthesis of single-crystal silver nanowires through a tannin-reduction process," *Journal of Nanoparticle Research*, 2009. **11**(7): p. 1839-1844.

10.   Chen, M., Y.-G. Feng, X. Wang, T.-C. Li, J.-Y. Zhang, and D.-J. Qian, "Silver Nanoparticles Capped by Oleylamine: Formation, Growth, and Self-Organization," *Langmuir*, 2007. **23**(10): p. 5296-5304.

11.   Ahmad, A., P. Mukherjee, S. Senapati, D. Mandal, M.I. Khan, R. Kumar, and M. Sastry, "Extracellular biosynthesis of silver nanoparticles using the fungus Fusarium oxysporum," *Colloids and Surfaces B: Biointerfaces*, 2003. **28**(4): p. 313-318.

12.   Deng, Z., M. Mansuipur, and A.J. Muscat, "New Method to Single-Crystal Micrometer-Sized Ultra-Thin Silver Nanosheets: Synthesis and Characterization," *The Journal of Physical Chemistry C*, 2008. **113**(3): p. 867-873.

13.   Tolaymat, T.M., A.M. El Badawy, A. Genaidy, K.G. Schekel, T.P. Luxton, and M. Suidan, "An evidence-based environmental perspective of manufactured silver nanoparticle in syntheses and applications: A systematic review and critical appraisal of peer-reviewed scientific papers," *Science of The Total Environment*. **In Press, Corrected Proof**.

14.   Olenin, A., Y. Krutyakov, A. Kudrinskii, and G. Lisichkin, "Formation of surface layers on silver nanoparticles in aqueous and water-organic media," *Colloid Journal*, 2008. **70**(1): p. 71-76.

15.   Yamamoto, M., Y. Kashiwagi, and M. Nakamoto, "Size-Controlled Synthesis of Monodispersed Silver Nanoparticles Capped by Long-Chain Alkyl Carboxylates from Silver

Carboxylate and Tertiary Amine," *Langmuir*, 2006. **22**(20): p. 8581-8586.

16. Zheng, N., J. Fan, and G.D. Stucky, "One-Step One-Phase Synthesis of Monodisperse Noble-Metallic Nanoparticles and Their Colloidal Crystals," *Journal of the American Chemical Society*, 2006. **128**(20): p. 6550-6551.

17. Xu, Z., C. Shen, Y. Hou, H. Gao, and S. Sun, "Oleylamine as Both Reducing Agent and Stabilizer in a Facile Synthesis of Magnetite Nanoparticles," *Chemistry of Materials*, 2009. **21**(9): p. 1778-1780.

18. Wu, H., J. Xu, X. He, Y. Zhao, and H. Wen, "Mesoscopic simulation of self-assembly in surfactant oligomers by dissipative particle dynamics," *Colloids and Surfaces A: Physicochemical and Engineering Aspects*, 2006. **290**(1-3): p. 239-246.

19. Mohammad A., H.S., "Use of sodium bis (2-ethyl hexyl) sulfosuccinate (AOT) anionic surfactant mobile phase systems in thin-layer chromatography of amino acids: simultaneous separation of thioamino acids," *Chromatography*, 2004. **24**(5): p. 111-118.

20. Karakoc, N., *Metal polymer composite nanofiber production by electrospinning*, in *Chemical Engineering*. 2009, Middle East Technical University: Ankara. p. 95.

21. Shon, Y.-S. and E. Cutler, "Aqueous Synthesis of Alkanethiolate-Protected Ag Nanoparticles Using Bunte Salts," *Langmuir*, 2004. **20**(16): p. 6626-6630.

22. Yin, H., T. Yamamoto, Y. Wada, and S. Yanagida, "Large-scale and size-controlled synthesis of silver nanoparticles under microwave irradiation," *Materials Chemistry and Physics*, 2004. **83**(1): p. 66-70.

23.   Ghosh, D. and S. Dasgupta, "Synthesis of Submicron Silver Powder by the Hydrometallurgical Reduction of Silver Nitrate with Hydrazine Hydrate and a Thermodynamic Analysis of the System," *Metallurgical and Materials Transactions B*, 2008. **39**(1): p. 35-45.

24.   Canamares, M.V., J.V. Garcia-Ramos, J.D. Gomez-Varga, C. Domingo, and S. Sanchez-Cortes, "Comparative Study of the Morphology, Aggregation, Adherence to Glass, and Surface-Enhanced Raman Scattering Activity of Silver Nanoparticles Prepared by Chemical Reduction of Ag^+ Using Citrate and Hydroxylamine," *Langmuir*, 2005. **21**(18): p. 8546-8553.

25.   Leopold, N. and B. Lendl, "A New Method for Fast Preparation of Highly Surface-Enhanced Raman Scattering (SERS) Active Silver Colloids at Room Temperature by Reduction of Silver Nitrate with Hydroxylamine Hydrochloride," *The Journal of Physical Chemistry B*, 2003. **107**(24): p. 5723-5727.

26.   Li, Y., Y. Ding, and Z. Wang, "A Novel Chemical Route to ZnTe Semiconductor Nanorods," *Advanced Materials*, 1999. **11**(10): p. 847-850.

27.   Hou, Y., Z. Xu, and S. Sun, "Controlled Synthesis and Chemical Conversions of FeO Nanoparticles," *Angewandte Chemie International Edition*, 2007. **46**(33): p. 6329-6332.

28.   Mazumder, V. and S. Sun, "Oleylamine-Mediated Synthesis of Pd Nanoparticles for Catalytic Formic Acid Oxidation," *Journal of the American Chemical Society*, 2009. **131**(13): p. 4588-4589.

29.   Chiang, I.-C. and D.-H. Chen, "Structural characterization and self-assembly into superlattices of iron oxide–gold core–shell nanoparticles synthesized via a high-temperature organometallic route," *Nanotechnology*, 2009. **20**(1): p. 015602.

30. de la Presa, P., M. Multigner, J. de la Venta, M.A. Garcia, and M.L. Ruiz-Gonzalez, "Structural and magnetic characterization of oleic acid and oleylamine-capped gold nanoparticles," *Journal of Applied Physics*, 2006. **100**(12): p. 123915-6.

31. Klokkenburg, M., J. Hilhorst, and B.H. Erné, "Surface analysis of magnetite nanoparticles in cyclohexane solutions of oleic acid and oleylamine," *Vibrational Spectroscopy*, 2007. **43**(1): p. 243-248.

32. Song, T., Y. Zhang, T. Zhou, C.T. Lim, S. Ramakrishna, and B. Liu, "Encapsulation of self-assembled FePt magnetic nanoparticles in PCL nanofibers by coaxial electrospinning," *Chemical Physics Letters*, 2005. **415**(4-6): p. 317-322.

33. Lu, X., M.S. Yavuz, H.-Y. Tuan, B.A. Korgel, and Y. Xia, "Ultrathin Gold Nanowires Can Be Obtained by Reducing Polymeric Strands of Oleylamine−AuCl Complexes Formed via Aurophilic Interaction," *Journal of the American Chemical Society*, 2008. **130**(28): p. 8900-8901.

34. Lo, H., S. Kadiyala, S.E. Guggino, and K.W. Leong, "Poly(L-lactic acid) foams with cell seeding and controlled-release capacity," *Journal of Biomedical Materials Research*, 1996. **30**(4): p. 475-484.

35. Frenot, A. and I.S. Chronakis, "Polymer nanofibers assembled by electrospinning," *Current Opinion in Colloid & Interface Science*, 2003. **8**(1): p. 64-75.

36. Hartgerink, J.D., E. Beniash, and S.I. Stupp, "Self-Assembly and Mineralization of Peptide-Amphiphile Nanofibers," *Science*, 2001. **294**(5547): p. 1684-1688.

37. Harfenist, S.A., S.D. Cambron, E.W. Nelson, S.M. Berry, A.W. Isham, M.M. Crain, K.M. Walsh, R.S. Keynton, and R.W. Cohn, "Direct Drawing of Suspended Filamentary Micro- and

Nanostructures from Liquid Polymers," *Nano Letters*, 2004. **4**(10): p. 1931-1937.

38.   Christopherson, G.T., H. Song, and H.-Q. Mao, "The influence of fiber diameter of electrospun substrates on neural stem cell differentiation and proliferation," *Biomaterials*, 2009. **30**(4): p. 556-564.

39.   Huang, Z.-M., Y.Z. Zhang, M. Kotaki, and S. Ramakrishna, "A review on polymer nanofibers by electrospinning and their applications in nanocomposites," *Composites Science and Technology*, 2003. **63**(15): p. 2223-2253.

40.   Huang, Z.-M., Y.Z. Zhang, S. Ramakrishna, and C.T. Lim, "Electrospinning and mechanical characterization of gelatin nanofibers," *Polymer*, 2004. **45**(15): p. 5361-5368.

41.   Kenawy, E.-R., F.I. Abdel-Hay, M.H. El-Newehy, and G.E. Wnek, "Processing of polymer nanofibers through electrospinning as drug delivery systems," *Materials Chemistry and Physics*, 2009. **113**(1): p. 296-302.

42.   Andrady, A.L., *Science and Technology of Polymer Nanofibers* 2008, New Jersey: Wiley, John & Sons, Inc. 404.

43.   Zhenyu Li, H.H.C.W., "Electrostatic Forces Induce Poly(vinyl alcohol)-Protected Copper Nanoparticles to Form Copper/Poly(vinyl alcohol) Nanocables via Electrospinning," *Macromolecular Rapid Communications*, 2006. **27**(2): p. 152-155.

44.   Jeon, H.J., J.S. Kim, T.G. Kim, J.H. Kim, W.-R. Yu, and J.H. Youk, "Preparation of poly([var epsilon]-caprolactone)-based polyurethane nanofibers containing silver nanoparticles," *Applied Surface Science*, 2008. **254**(18): p. 5886-5890.

45.   Hong, K.H., J.L. Park, I.H. Sul, J.H. Youk, and T.J. Kang, "Preparation of antimicrobial poly(vinyl alcohol) nanofibers containing silver nanoparticles," *Journal of Polymer Science Part B: Polymer Physics*, 2006. **44**(17): p. 2468-2474.

46.   Moghe, A.K. and B.S. Gupta, "Co-axial Electrospinning for Nanofiber Structures: Preparation and Applications," *Polymer Reviews*, 2008. **48**(2): p. 353 - 377.

47.   Li, D. and Y. Xia, "Direct Fabrication of Composite and Ceramic Hollow Nanofibers by Electrospinning," *Nano Letters*, 2004. **4**(5): p. 933-938.

48.   Sun, Z., E. Zussman, A.L. Yarin, J.H. Wendorff, and A. Greiner, "Compound Core-Shell Polymer Nanofibers by Co-Electrospinning," *Advanced Materials*, 2003. **15**(22): p. 1929-1932.

49.   Yu, J.H., S.V. Fridrikh, and G.C. Rutledge, "Production of Submicrometer Diameter Fibers by Two-Fluid Electrospinning," *Advanced Materials*, 2004. **16**(17): p. 1562-1566.

50.   Sun, B., B. Duan, and X. Yuan, "Preparation of core/shell PVP/PLA ultrafine fibers by coaxial electrospinning," *Journal of Applied Polymer Science*, 2006. **102**(1): p. 39-45.

51.   Stewart, M.E., C.R. Anderton, L.B. Thompson, J. Maria, S.K. Gray, J.A. Rogers, and R.G. Nuzzo, "Nanostructured Plasmonic Sensors," *Chemical Reviews*, 2008. **108**(2): p. 494-521.

52.   Zhang, W., X. Qiao, and J. Chen, "Synthesis of silver nanoparticles--Effects of concerned parameters in water/oil microemulsion," *Materials Science and Engineering: B*, 2007. **142**(1): p. 1-15.

APPENDIX A

MATERIALS

Materials used in the experiments were listed at TableA1. This table also includes the structures and properties of these materials.

Table A.1 List of chemicals
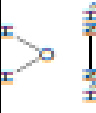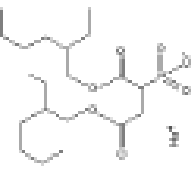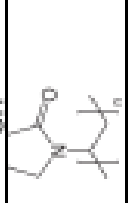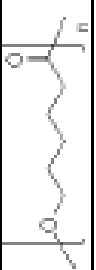
Chemical	Chemical Formula	Chemical Structure	Molecular Weight (g/mol)	Density (g/ml)	Purity	Firm
Silver Nitrate	$AgNO_3$		169.87	-	extra pure	Merck
Hydrazine Hydrate	$N_2H_4 \cdot H_2O$		50.06	1.0045	80%	Merck
Dioctyl Sulfosuccinate Sodium Salt	$C_{20}H_{37}O_7SNa$		444.56		98%	Sigma Aldrich
Oleylamine	$C_{18}H_{37}N$		267.50	0.813	70%	Sigma Aldrich
Oleic Acid	$C_{18}H_{34}O_2$		282.46	0.895	Tech. grade	Riedel-de-Haen

Table A.1 List of chemicals (continued)

Chemical	Chemical Formula	Chemical Structure	Molecular Weight (g/mol)	Density (g/ml)	Purity	Firm
Polyvinyl Alcohol	$(CH_2OH)_n$		23,000	-	100%	Clariant
Polyvinyl Pyrrolidone	$(C_6H_9NO)_n$		1,300,000	-	100%	Sigma Aldrich
Polycaprolactone	$(C_6H_{10}O_2)_n$		80,000	-	100%	Sigma Aldrich
N-Hexane	C_6H_{14}		86.18	0.66	≥95.0	Merck
Ethanol	C_2H_6O		46.07	0.789	≥99.8	Sigma Aldrich
N,N-Dimethyl formamide	C_3H_7NO		73.10	0.94	≥99.8	Merck
2,2,2-Triflouroethanol	$C_2H_3F_3O$		100.04	1.38	≥99.0	Merck

APPENDIX B

PARTICLE SIZE CALCULATION FROM XRD DATA

Optimized solution was used as an example of this calculation. XRD pattern of almost perfect crystalline particles were used to estimate error comes from the diffractometer. FWHM value of the most intense peak of this pattern was estimated 0.137°. After that four peaks of the silver particles were deconvoluted and FWHM values of each were estimated approximately 5.4°.

Correcting FWHM value can be calculated from the Equation 2.7.

$$B_{1/2}^2 = B_{obs}^2 - B_m^2 \tag{2.7}$$

$$B_{1/2}^2 = 5.4^2 - 0.137^2 = 29.4$$

$$B_{1/2} = 5.42° = 5.42 \times \frac{\pi}{180°} = 0.095 rad$$

For the most intense peak of the silver particles (2θ=38.55°)

$$\cos\theta = \cos\left(\frac{38.55}{2}\right) = 0.94$$

For the K values of 0.89 and λ value of 1.5406Å;

$$<L>_{vol} = \frac{K\lambda}{B_{1/2}\cos\theta_B} = \frac{0.89 \times 1.5406Å}{0.095 \times 0.94} = 15.3Å = 1.53nm$$

Table B.1 is the list of particle sizes calculated by Scherrer Equation

<center>

Table B.1 Particle sizes by Scherrer Equation.

Sample	Particle Size (nm)
OS	1.5
OS at 150°C	1.7
sonication but no mixing	2.0
OS, 50min reaction	1.7
0.235M AgNO$_3$, 1.2M OAm, 0.7M OAc	1.5
0.288M AgNO$_3$, 1.4M OAm, 0.1M OAc	1.6
0.039M AgNO$_3$, 1.2M OAm, 0.7M OAc	1.5

</center>

APPENDIX C

RESULTS FOR HYDRAZINE HYDRATE SYSTEM
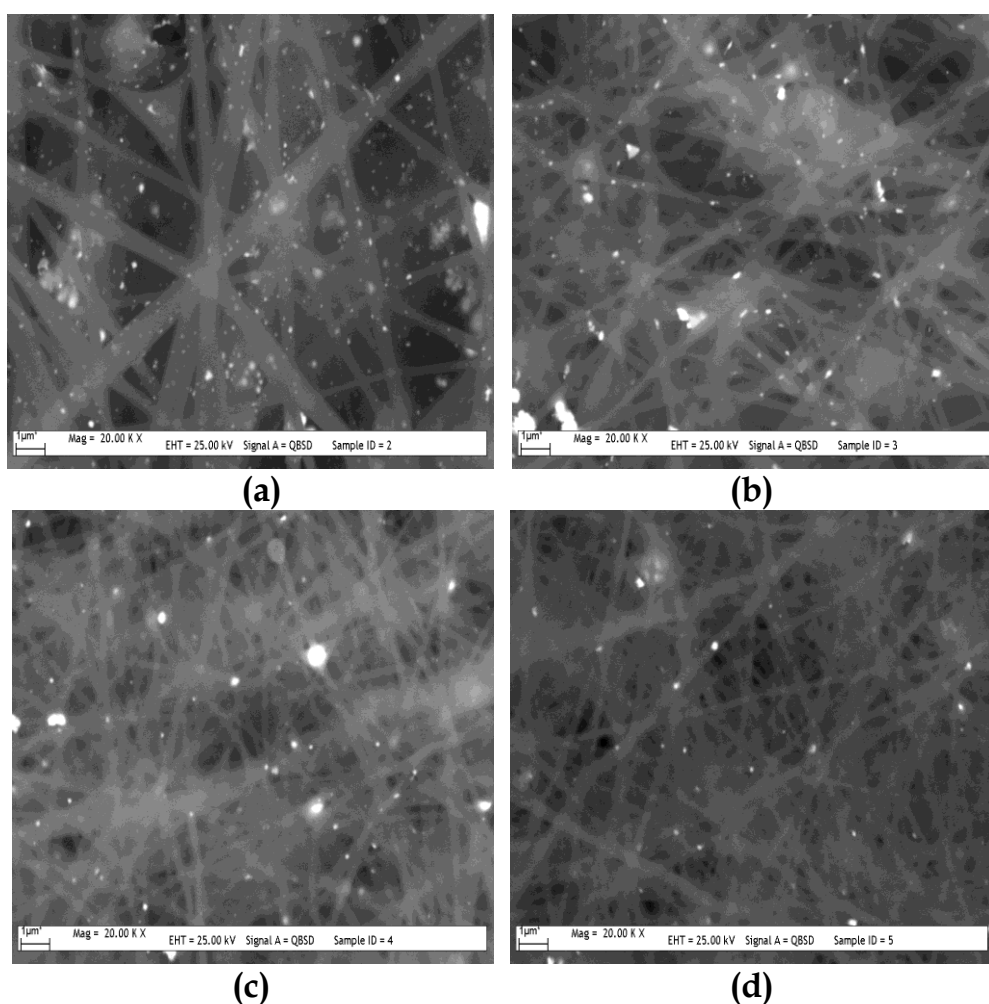
Figure C.1 Effects of different DSS amounts; (a) 2×CMC, (b) 4×CMC, (c) 6×CMC, (d) 8×CMC.

Changes in amount of surfactant could not prevent agglomeration. As seen in Figure C.1, sizes of the particles were distributed in wide range.
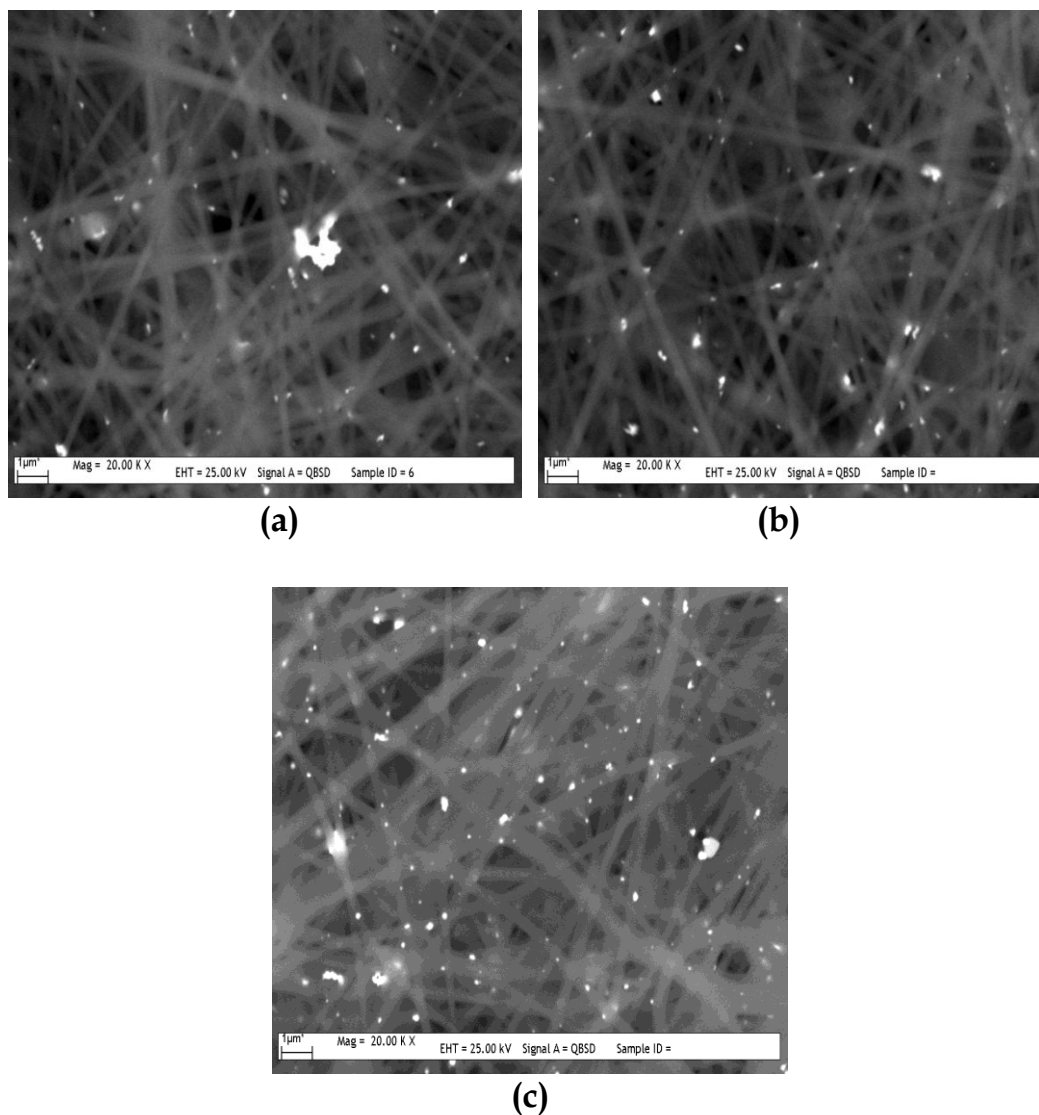

(a)

(b)

(c)

Figure C.2 Effect of PVA amount; (a) 2.4g, (b) 2.6g, and (c) 2.8g.

For the values below 2.4g, solution was too dilute solution to electrospin. For the values 2.4g, viscosity began to increase and diameter of the fibers increase as expected. However, this parameter

also cannot change the situation and particles stayed as relatively big clusters.
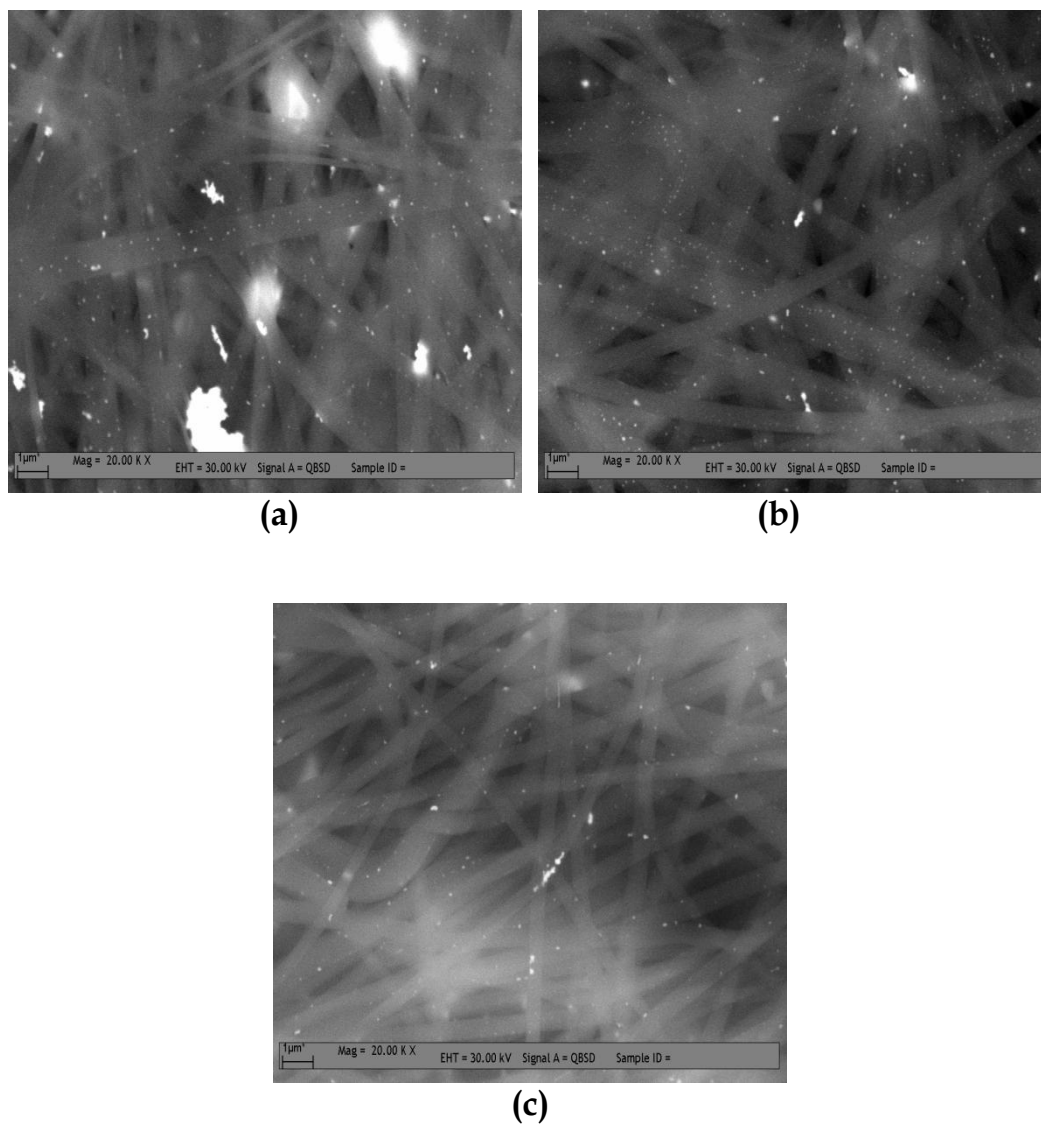
Figure C.3   Effect of HH to AgNO$_3$ ratios; (a) 5.0, (b) 6.0, and (c) 7.0.

As mentioned in 'Results and Discussion' section, increase in the HH to silver nitrate ratio does not affect the particle size distribution too much.
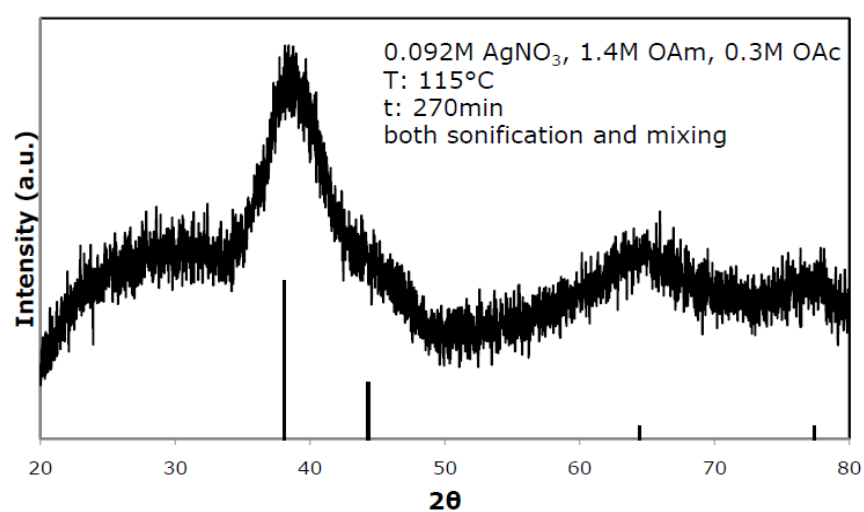
APPENDIX D

XRD RESULTS

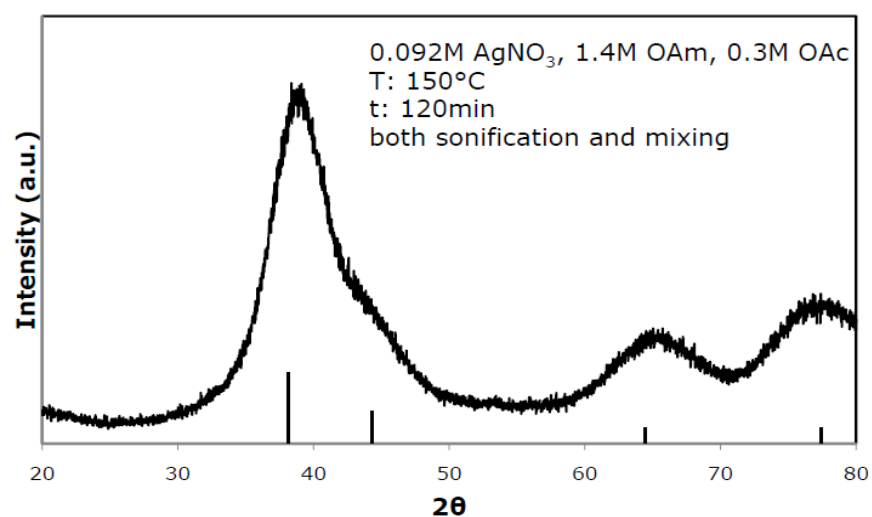**Figure D.1** XRD pattern of typical solution with 4.5h reaction time.

Figure D.2 XRD pattern of typical solution with reaction temperature of 150°C
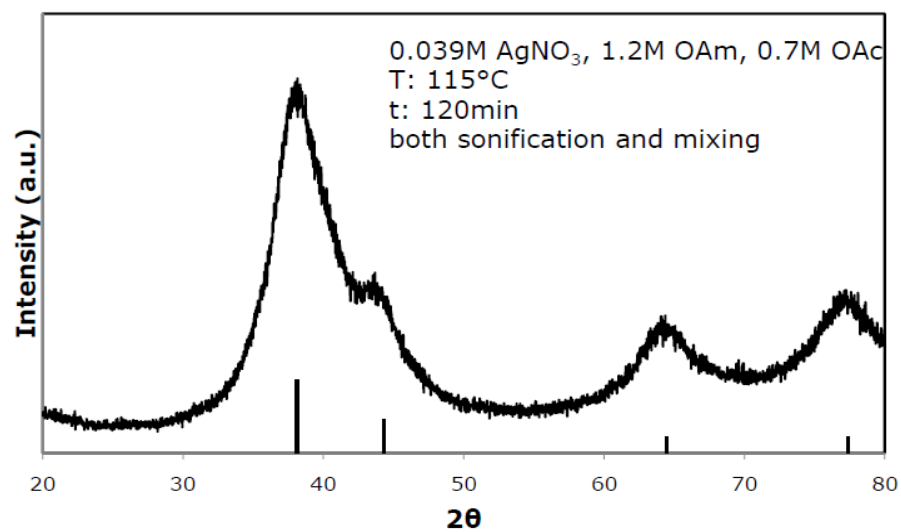
Figure D.3 XRD pattern of typical solution with the concentration of 0.039M AgNO3, 1.2M OAm, 0.7M OAc
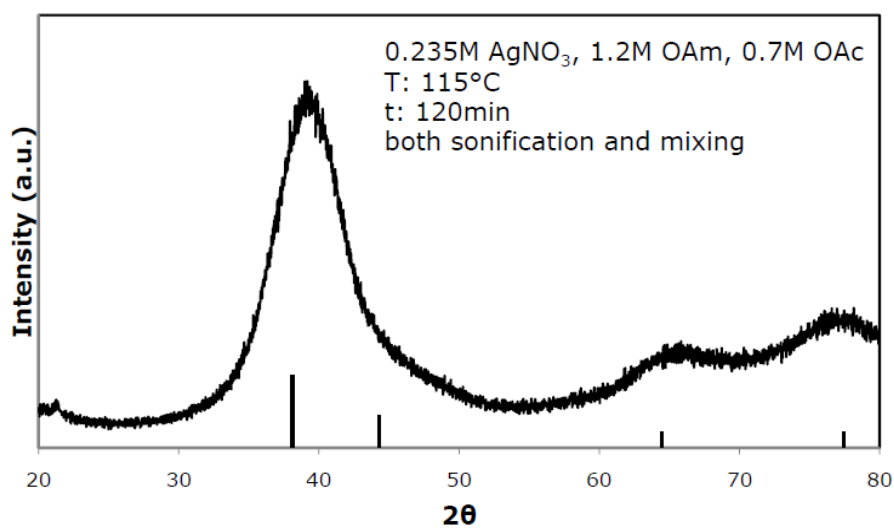

Figure D.4 XRD pattern of typical solution with the concentration of 0.235M AgNO3, 1.2M OAm, 0.7M OAc
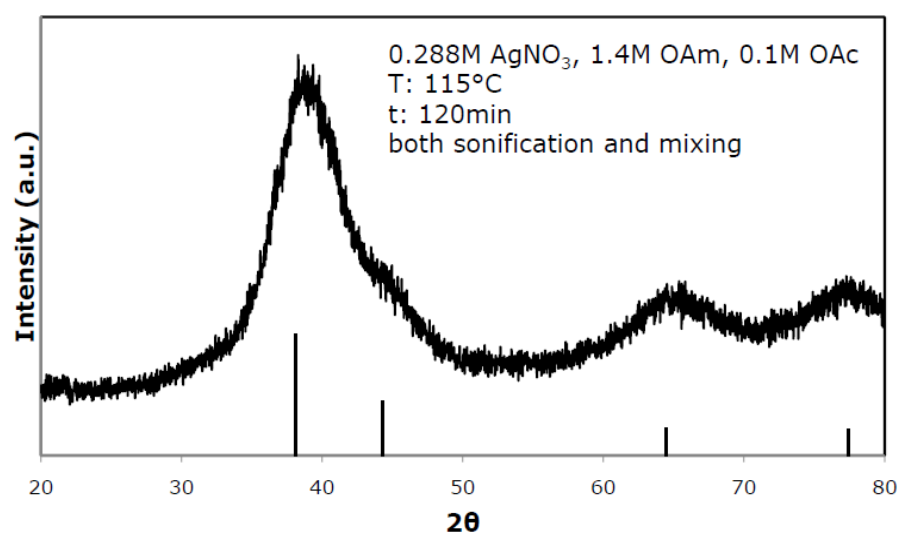
Figure D.5 XRD pattern of typical solution with the concentration of 0.288M AgNO3, 1.4M OAm, 0.1M OAc